Gondwana Research 140 (2025) 17–33

Contents lists available at ScienceDirect

Gondwana Research

journal homepage: www.elsevier.com/locate/gr

# Sedimentary provenance analysis by coupled detrital zircon U-Pb, Hf isotopes of the Paleoproterozoic Belcher Group, Nunavut, Canada and implications for sedimentation during the opening and closure of the Manikewan Ocean

Brayden S. McDonald *, Camille A. Partin

*University of Saskatchewan, Department of Geological Sciences, Saskatoon, SK S7N 5E2, Canada*

ARTICLE INFO

Handling Editor: A. Festa

*Keywords:*
U-Pb geochronology
Hf isotopes
Superior craton
Trans-Hudson orogen
Canadian shield

ABSTRACT

Coupled detrital zircon U-Pb, Hf isotopic data from the Paleoproterozoic Belcher Group, Nunavut, Canada, are presented to determine maximum depositional ages and sedimentary provenance. We use these data to evaluate potential sediment sources with matching ages and εHf values within a paleogeographic context, to better define the configuration of microcontinents, terranes, and cratons surrounding the Belcher basin during its deposition. The distribution of detrital zircon spectra show that the lower Belcher Group was deposited on the passive margin of the Superior craton, whereas the upper Belcher Group (Omarolluk and Loaf formations) was deposited in *syn*-orogenic phase, broadly reflecting the opening and closing stages of the Manikewan Ocean, respectively. The lower Belcher Group data show dominant detrital zircon populations between 2825 and 2690 Ma (associated with negative εHf values) with only minor detrital input from sources < 2100 Ma. The dominant grain population is interpreted to be derived from the northeastern Superior craton (>2680 Ma grains), and the Winnipeg River and North Caribou terranes (<2680 Ma grains). The upper Belcher Group shows a dramatic shift in detrital ages from Archean to dominantly Paleoproterozoic, with dominant age peaks between ca. 1920 and 1900 Ma and only minor Archean input that includes 2500 Ma sources that are absent in the lower units. Archean populations document Sask craton-like ages and εHf values, whereas the dominant detrital 1920 to 1900 Ma age population shows positive εHf values that are consistent with being sourced from terranes located in the western Reindeer zone deposited in a submarine fan.

## 1. Introduction

Sedimentary provenance studies are essential to decipher detrital source areas and the pathways by which those sediments travel from source to sink. This is particularly important for understanding the timing of accretionary and collisional tectonic events and the history of the amalgamation of supercontinents, although this task becomes more challenging in older (e.g., Paleoproterozoic) sedimentary units. Utilizing coupled detrital zircon U-Pb geochronology and Lu-Hf isotopes as a tool to determine provenance is essential in assessing the tectonic setting of the basin during sedimentation, as well as uncovering the paleogeography of surrounding cratons that were source areas.

Situated along the margin of the Superior craton of the Canadian Shield (Fig. 1), the Paleoproterozoic Belcher Group offers an opportunity to gain insights into sedimentary deposition during the opening and closing of the Manikewan Ocean—the latter of which was the result of the ca. 1.8 Ga Trans-Hudson orogen. The Trans-Hudson orogen stands out as a formative event in the amalgamation of the Canadian Shield that in part led to the formation of the supercontinent, Nuna. The details of ca. 1.92 to 1.83 Ga accretionary and collisional orogenic events can be deduced from the geological framework of volcanic island arcs, plutonic rocks, and sedimentary basins that formed along the margins of cratons involved in the terminal collision between the Superior craton, Trans-Hudson orogen internides, and the Churchill province (e.g., Hoffman, 1988; Ansdell, 2005; Corrigan et al., 2009). Deposition of the Belcher Group began ca. 2020 Ma (Hodgskiss et al., 2019) and continued until ca. 1830 (Corrigan et al., 2021), thus overlapping with the opening and closing stages of the Manikewan Ocean.

* Corresponding author.
*E-mail address:* brayden.mcdonald@usask.ca (B.S. McDonald).

https://doi.org/10.1016/j.gr.2025.01.004
Received 9 August 2024; Received in revised form 30 November 2024; Accepted 3 January 2025
Available online 5 January 2025

The Belcher Group is composed of seven to ten kilometers of carbonate, siliciclastic, and volcanic rocks that were not subjected to deep burial or intense deformation during the Trans-Hudson orogen (Jackson, 2013). Consequently, the stratigraphy and sedimentary structures of the Belcher Group are well-preserved, allowing for the reconstruction of depositional environments (e.g., Ricketts, 1979), as well as the preservation of the oldest cyanobacterial fossils (Demoulin et al., 2019; Hofmann, 1976). The lower and middle Belcher Group formations, which account for greatest proportion of the stratigraphy (Kasegalik to Kipalu formations), principally reflect deposition along a passive margin that developed following a period of rifting during deposition of the Kasegalik Formation (Hodgskiss et al., 2019) and emplacement of the Eskimo volcanic rocks. Conversely, the upper Belcher Group formations (Omarolluk and Loaf) reflect deposition during the closure of the Manikewan Ocean. As a result, the upper Belcher Group is composed of > 3.1-kilometer-thick sedimentary gravity flow deposits and deeper-water facies of the Omarolluk Formation, overlain by cross-bedded sandstone and intraformational conglomerate documenting a shift towards terrestrial sedimentation of the Loaf Formation (Ricketts and Donaldson, 1981). A reversal in paleoslope during the transition from passive margin to foreland basin sedimentation (Ricketts, 1979, 1981) predicts a shift in sediment provenance between the lower and upper Belcher Group. Previous work reported detrital zircon U-Pb data from the Kasegalik, Mukpollo, and lower Loaf formations (Corrigan et al., 2021; Hodgskiss et al., 2019), as well as zircon U-Pb ages from tuff beds in the Kasegalik and Omarolluk formations (Hodgskiss et al., 2019) that provide important constraints on depositional age.

Here, we present the first systematic, database-driven provenance analysis of the Belcher Group. Through a combination of zircon U-Pb and Hf isotope data, we compare potential source areas to delineate dominant sediment sources for the Belcher Group formations. Our new coupled detrital zircon U-Pb, Hf data from the Costello, Omarolluk, and Loaf formations are combined with previous detrital zircon U-Pb geochronology data to show a progression of age spectra for the lower, middle, and upper Belcher Group and define potential source areas to understand the paleogeographic context of the surrounding the Belcher basin during the deposition of the studied units.

## 2. Geological framework

### 2.1. Stratigraphy and age constraints of the Belcher Group

The Orosirian (2050–1800 Ma) Belcher Group is located approximately 150 km off the shore of western Québec in southeast Hudson Bay in Nunavut, Canada, and is exposed as a sinuous archipelago that constitutes the Belcher Islands (Fig. 2). The Belcher Group contains 14 sedimentary and volcanic formations (Fig. 3) representing a ~ 185-million-year depositional window (ca. 2020 Ma to 1830 Ma) during the amalgamation of proto-Laurentia and other parts of the Canadian Shield. The seven to 10 km thick package can be divided into six depositional phases (Ricketts, 1979), which capture the tectonic evolution of the Superior craton margin and the environmental transition from a transgressive carbonate platform to deeper marine to meandering rivers (Ricketts, 1981, 1981; Ricketts and Donaldson, 1988). From base

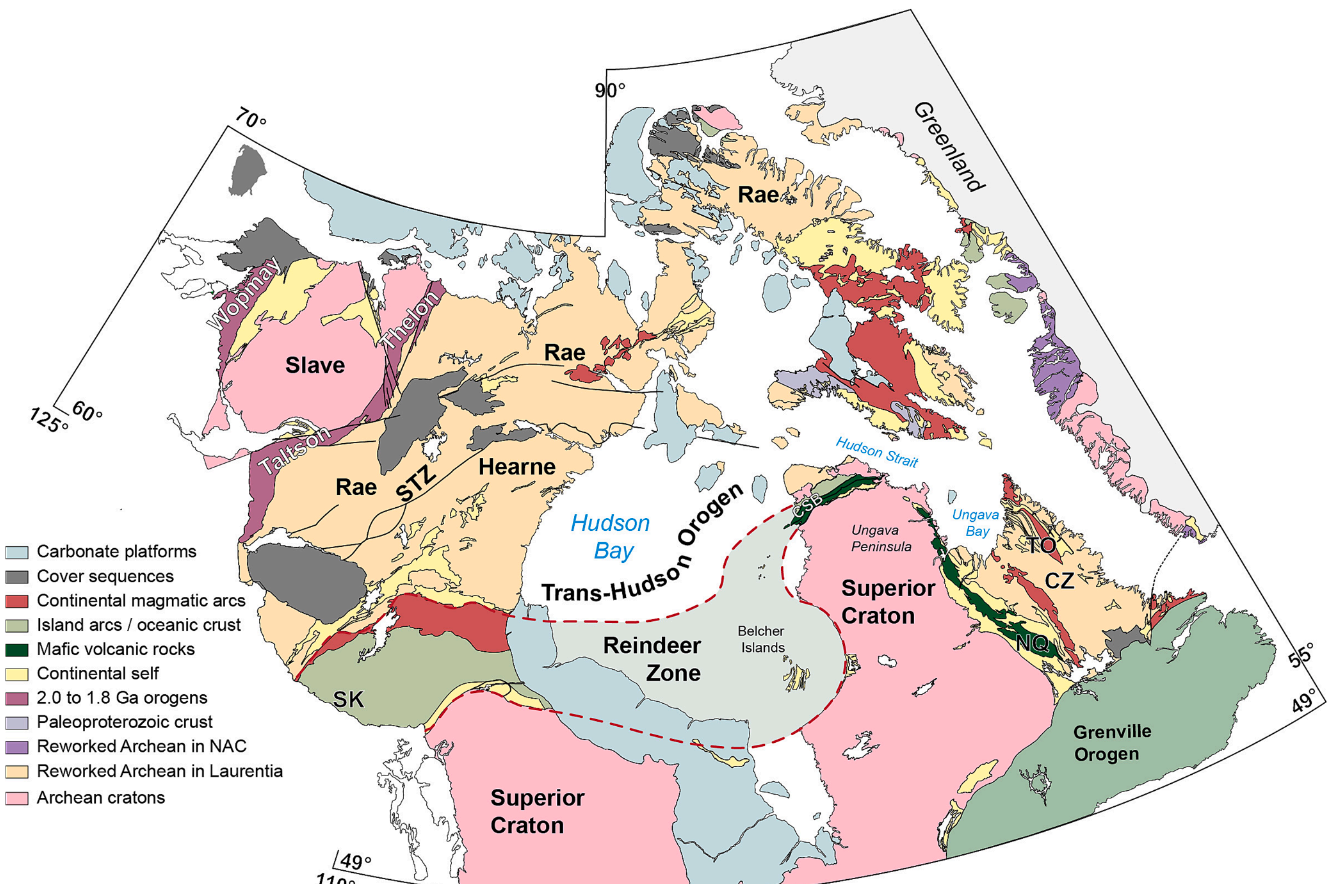


**Fig. 1.** Simplified geological map of the Canadian Shield and West Greenland showing the distribution of Archean cratons, Paleoproterozoic terranes and supracrustal rocks, and Phanerozoic rocks. The red dashed lines outline the Reindeer zone and Trans-Hudson internides. Modified after Corrigan et al. (2009). Greenland is shown in a pre-late Cretaceous position with respect to Canada. Abbreviations: CSB, Cape Smith fold belt; CZ, Core Zone; NQ, New Québec orogen; STZ, Snowbird Tectonic Zone; TO, Torngat orogen; SK, Sask craton. (For interpretation of the references to color in this figure legend, the reader is referred to the web version of this article.)

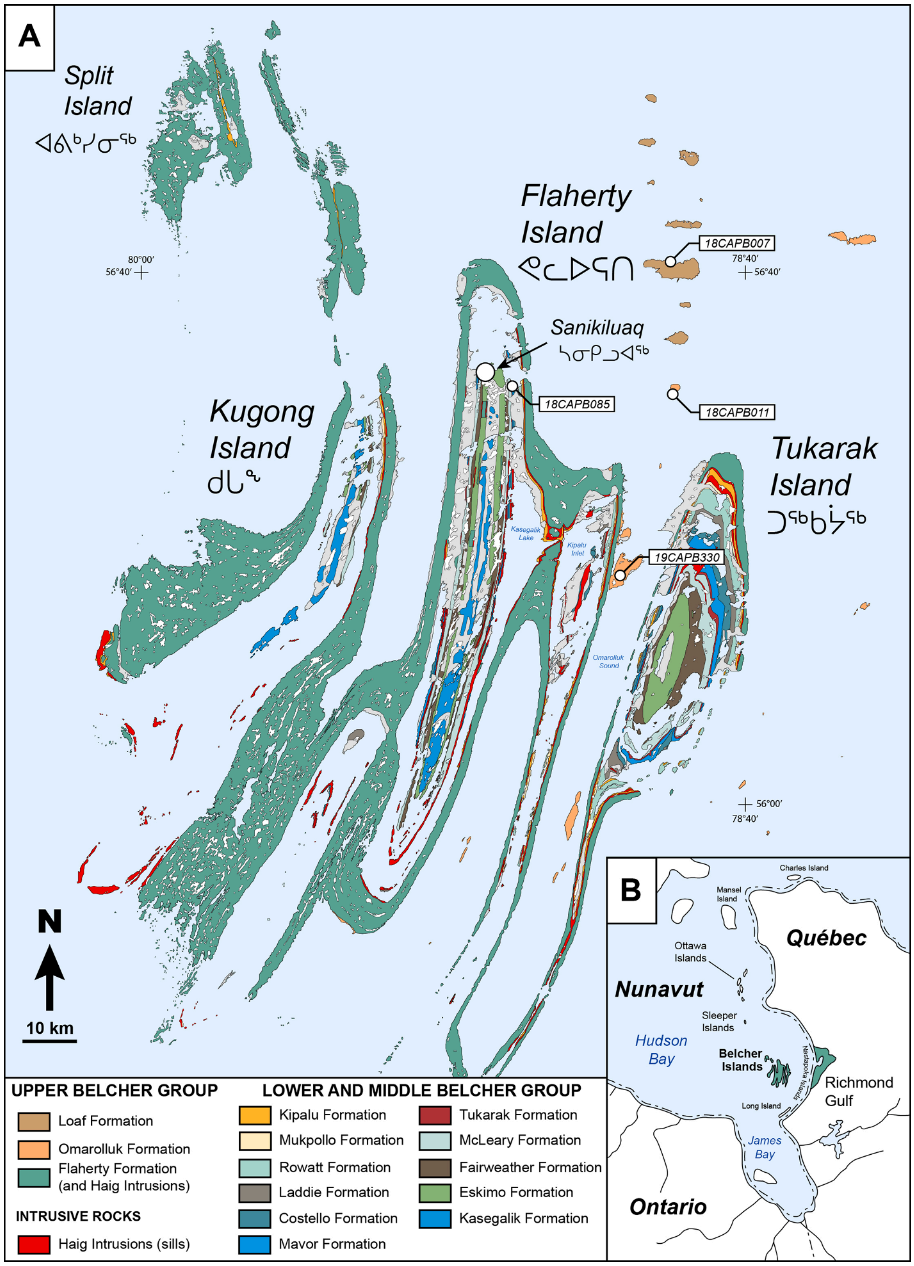


**Fig. 2.** A) Geological map of the Belcher Islands, Nunavut, Canada, and locations of samples analyzed in this study. The names of major islands and the community of Sanikiluaq also listed in Inuktitut. Modified after McDonald and Partin (2024) based on the geological map of Jackson (2013). B) Location of the Belcher Islands within the Hudson Bay region in central Canada.

to top the formations are: Kasegalik, Eskimo, Fairweather, McLeary, Tukarak, Mavor, Costello, Laddie, Rowatt, Mukpollo, Kipalu, Flaherty, Omarolluk, and Loaf formations. A detailed account of the stratigraphy and geological setting of the Belcher Group can be found in Jackson (2013), Hodgskiss et al. (2019), and McDonald and Partin (2024). We briefly summarize the stratigraphy here, focusing mainly on the studied units.

The lowermost Kasegalik Formation, which accounts for more than 1.1 km of stratigraphy is characterized by a seaward migration of depositional environments, moving away from sabkha-like marginal marine conditions with gypsum pseudomorphs and halite casts to shallow tidal environments dominated by stromatolitic dolostone near the top (Jackson, 2013; Ricketts, 1983; Ricketts and Donaldson, 1988). A collection of microfossils from the upper Kasegalik Formation were identified by Hoffman (1976) including *Eoentophysalis belcherensis*, the oldest known fossil occurrence of cyanobacterial cells. Zircon dating of two tuffaceous beds near the top and bottom of the formation by Hodgskiss et al. (2019) yielded U-Pb ages of 2018.5 ± 1.0 Ma and 2015.4 ± 1.8 Ma, respectively, which places initial deposition of the Kasegalik Formation at ca. 2018 Ma and suggests that sedimentation continued until ca. 2015 Ma (Hodgskiss et al., 2019). Deposition of the Kasegalik Formation ceased shortly after ca. 2015 Ma and was followed by a series of tholeiitic basalt flows of the 200- to 1000-m thick Eskimo Formation that are ascribed to a period of continental flood basalt attributed to rifting along the western margin of the Superior craton (Jackson, 1960; Legault et al., 1994). Following the Eskimo flood basalt, renewed sedimentation ushered in passive margin deposition with the development of a transgressive carbonate platform that defines the bulk of the lower and middle Belcher Group. The earliest stages of platform buildup are defined by sandstone and siltstone facies with a series of shoaling upwards cycles dominated by pisolitic dolostone facies of the Fairweather Formation (~300 to 600 m thick). The McLeary Formation

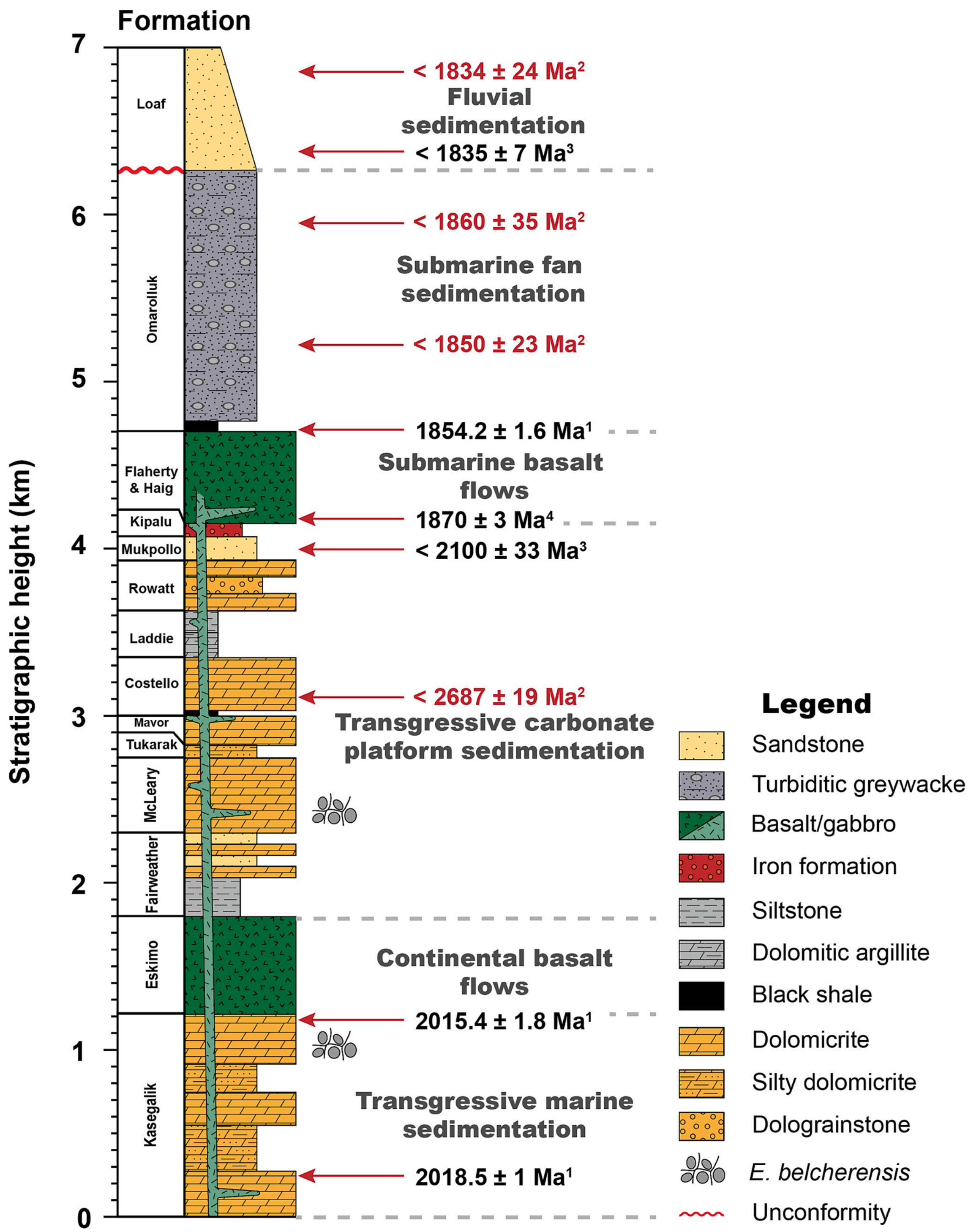


**Fig. 3.** Simplified stratigraphic column of the Belcher Group with generalized depositional phases outlined (modified from McDonald and Partin, 2024). Associated U-Pb ages are shown at approximate stratigraphic height. U-Pb ages are from: (1) Hodgskiss et al. (2019), (2) this study. (3) Corrigan et al. (2021), and (4) Hamilton et al. (2009).

conformably overlies the Fairweather Formation and is a ~ 250- to 470-meter-thick formation composed of dolomicrite and stromatolitic dolostone facies, showing a progression from intertidal to a fully subtidal environment. The McLeary Formation also contains microfossils including *Eoentophysalis belcherensis* (Hofmann, 1976; Morrow-Pollock, 2021). Following the tidal environment of the McLeary Formation, the Tukarak Formation is characterized by ~ 100 m of thin-bedded to laminated, maroon colored, dolomicritic siltstone and red argillite with a corrugated texture, interpreted to represent deposition along a muddy foreshore/shoreface environment that transitioned into the prograding carbonate reef complex of the Mavor Formation (Jackson, 2013; Ricketts, 1983). The Mavor Formation is defined by ~ 200 to 250 m of stratigraphy with a basal portion characterized by shoaling upwards cycles of dolomitic grainstone, followed by a series of increasingly more complex stromatolite mound structures (Ricketts and Donaldson, 1988; Sherman, 1994). The base of the overlying Costello Formation contains ~ 50 m of black to grey-black shale facies that transition into 250 to 370 m of rhythmically bedded dolomicritic siltstone facies, interpreted to represent deposition along a platform margin. The presence of intraformational conglomerate, slump folds and partial Bouma sequences, as well as horizons of calcite concretions found throughout support the interpretation of deposition along a slope (Jackson, 2013; Ricketts, 1979). The Costello Formation is directly overlain by the Laddie Formation, which contains a lower member of red colored shale with a minor dolomitic component and an upper member of grey-green siltstone. Dominance of siltstone facies and a smaller sandstone component led Ricketts (1979) and Ricketts and Donaldson (1988) to suggest deposition occurred below storm-weather wave base.

The next phase of deposition began with the Rowatt Formation (Fig. 3), a ~ 330-meter-thick sequence of sandstone and siltstone facies that grades into an upper member of dolomitic grainstone facies. The lower member is defined by a series of shallowing-up cycles and contains abundant cross-bedded sandstone, whereas the upper member contains evidence of minor channelization and soft-sediment deformation (Jackson, 2013). The overlying Mukpollo Formation is represented almost entirely by mature quartz arenite and ranges between 120 and 160 m thick. It contains desiccation cracks, straight-crested wave ripples, trough cross-beds and occasional channel structures filled with quartz arenite and is interpreted by Ricketts (1979) to represent an intertidal environment. The Kipalu Formation represents ~ 80 to 130 m of variably iron-rich argillite and lenses and nodular horizons of granular jasper (granular iron formation) with minor carbonate lithologies. The combination of thin-bedded siltstone and presence of granular iron formation led Ricketts (1979) to suggest deposition occurred within a restricted basin, which could have formed due to an increased input of ferrous iron into the oceans at this time (Rasmussen et al., 2012).

Deposition of the Kipalu Formation was followed by the emplacement of large volumes of tholeiitic submarine basalt flows of the Flaherty Formation and the feeder dykes of the Haig intrusions (Dimroth et al., 1970). The Flaherty Formation is largely composed of pillowed and massive basalt, mafic tuff, and minor volcaniclastic rocks. The formation varies in thickness (500 to 1600 m) across the Belcher Islands, but is thickest on the western edge of the islands (Ricketts et al., 1982). A baddeleyite U-Pb age of 1870 ± 3 Ma (Hamilton et al., 2009) from the Haig sills, which occur primarily at the base of the Flaherty Formation but also cross-cut every member of the lower stratigraphy, provides a minimum age constraint on all lower and middle Belcher Group units. The ca. 1870 Ma age supports the idea that the second phase of volcanism is linked to the development of volcanic arcs during the closing of the Manikewan Ocean during the Trans-Hudson orogen (e.g., Jackson, 2013). Alternatively, the Haig sills could be linked to a mantle plume associated with the Pan-Superior large igneous province (Ciborowski et al., 2017; Ernst and Bell, 2010). A tuffaceous shale located five meters above the base of the overlying Omarolluk Formation yielded a zircon U-Pb age of 1854.2 ± 1 Ma (Hodgskiss et al., 2019), placing a younger constraint on the timing of mafic volcanism. Importantly, it also provides a depositional age for the base of the Omarolluk Formation. The ~ 3,300 m-thick Omarolluk Formation is characterized by a lower member composed of repeating turbidite sequences deposited within a foreland basin that developed in response to collision along the promontories of the Superior craton. While the upper member is lithologically similar, it is dominated by thinly laminated to bedded greywacke facies with an abundance of both small scale (<5 cm) and large scale (>1.5 m) load and de-watering structures representing rapid deposition and/or slumping. The final stage of deposition is recorded by the > 675-meter-thick Loaf Formation. The Omarolluk-Loaf contact is not exposed but is assumed to be transitional by Ricketts (1979) based on interpreted lateral facies associations. The Loaf Formation is composed of fine-grained sandstone facies that record the transition from marine deposition to a fluvial-dominated environment. The upper member of the formation is characterized by fine- to medium grained reddish-pink arkose sandstone and occasional reworked dolomite facies. A youngest detrital zircon U-Pb age of 1835 ± 7 Ma (Corrigan et al., 2021) provides a maximum age constraint on the deposition of this unit. Paleocurrent indicators documented by Ricketts (1979) were interpreted to indicate a sediment source from a terrane located to the present-day northwest of the Belcher Islands (Ricketts and Donaldson, 1981). Following deposition of the Loaf Formation and during the final stages of the Trans-Hudson orogen, the Belcher Group underwent a single deformation event that resulted in isoclinal folding, where it reached a peak metamorphic grade of prehnite/pumpellyite facies (Jackson, 2013).

### 2.2. Regional geology

The geological history of the Belcher Group is linked to the history of the Manikewan Ocean. As the supercontinent Kenorland underwent protracted breakup between ca. 2.45 and 2.0 Ga (Aspler et al., 2001), the Superior craton developed thick passive margin sequences along one edge of the Manikewan Ocean. This includes the initiation of sedimentation starting at ca. 2.0 Ga of the Belcher Group, Richmond Gulf Group, and Povungnituk Group (Chandler and Parrish, 1989; Ricketts and Donaldson, 1981; St-Onge and Ijewliw, 1996; St-Onge and Lucas, 1991). Deposition of the Belcher Group records the development of thick carbonate platforms and shelf to slope environments. However, a dramatic change occurred as the regional tectonics shifted from ocean opening to ocean closing during phases of the ca. 1.9 to 1.8 Ga Trans-Hudson orogen (Corrigan et al., 2009; St-Onge et al., 2009).

The Hudson Bay region was the center of the terminal continent–continent collision between the Superior craton and Churchill Province (Rae and Hearne cratons). Closure of the Manikewan Ocean occurred over a 120-million-year period through a series of accretionary events that involved Paleoproterozoic ocean floor and back-arc volcanic rocks between Archean crustal blocks of the Rae-Hearne, Sask, and Superior cratons (Berman et al., 2007; Corrigan et al., 2021, 2009; Hoffman, 1981; St-Onge et al., 2006; Weller and St-Onge, 2017). The earliest stages of the Trans-Hudson orogen include the collision of the Rae and Hearne cratons during the Snowbird orogeny (ca. 1.92–1.89 Ga) and generation of juvenile arc terranes within the Manikewan Ocean (Ansdell, 2005). This was followed by a period of accretion including the La Ronge-Lynn Lake-Rusty Lake arcs colliding with the southeast margin of the Hearne craton during the Reindeer orogeny (ca. 1.88–1.865 Ga) and the formation of an interoceanic arc collage (Flin Flon-Glennie domain). Further east, the accretion of Meta Incognita to the eastern Rae craton was underway during the ca. 1.88 Ga Foxe orogeny (Corrigan et al., 2009). Massive volumes of mafic to ultramafic material were emplaced along the Superior craton margins forming the Circum-Superior belt (Baragar and Scoates, 1981) including the Molson dykes, Fox River sill, Haig intrusion in the Belcher Group, as well as the Chukotat sills in the Cape Smith belt. Emplacement of huge volumes of felsic plutonic rocks associated with the ca. 1.86–1.82 Ga Wathaman-Chipewyan and ca. 1.865 and 1.845 Ga Cumberland batholiths took place following the Foxe and Reindeer orogenies.

In Hudson Bay, the Severn arc is defined by an aeromagnetic anomaly in the middle of Hudson Bay and is interpreted as a continuation of the 1.86–1.82 Ga Chipewyan batholith, part of a north-dipping subduction system (Hoffman, 1990). This aeromagnetic anomaly merges with a southwest-trending positive Bouguer gravity anomaly that extends from the Sugluk block on land towards the center of Hudson Bay (Corrigan et al., 2021), and has also been called the Sugluk suture (Hoffman, 1990; Corrigan et al., 2021). The Sugluk block is an Archean microplate situated between Meta Incognita and the Superior craton and is present on the Ungava Peninsula as part of the gneissic suite of the Narsajuaq arc. However, prior to the collision between the Superior craton and the Sugluk block, the parautochthonous/autochthonous cover sequences of the ca. 2.04–1.96 Povungnituk and ca. 1.88–1.87 Ga Chukotat groups were folded and thrust imbricated along the Bergeron suture. These were then structurally overlain by ca. 1.92–1.86 Ga outboard juvenile arc terranes of the Parent and Spartan groups and the ca. 2.0 Ga oceanic crust of the Watts Group. The timing of terrane accretion represented by the Bergeron suture is important for our study. It is thought to have occurred as early as 1.87 Ga (Corrigan et al., 2021), or as late as 1.820 to 1.795 Ga (St-Onge et al., 2006). Collision of the Superior and Churchill Province along the Sugluk suture started at the Ungava Promontory at ca. 1.83 Ga, resulting in exhumation of the Sugluk block (Corrigan et al., 2021). The exhumation of the Sugluk block brought granulite facies crystalline basement rocks of the Churchill Province to surface and into contact with amphibolite facies rocks of the Superior craton (Corrigan et al., 2021). The collision and uplift of deeply buried Archean terranes is thought to be reflected in the sedimentary rock record of the Belcher Group, which contains Archean and Paleoproterozoic grains that are interpreted to be derived from intrusions of the Narsajuaq arc (Corrigan et al., 2021). Deposition of the upper Belcher Group formations documents a switch from passive margin to *syn*-collisional sedimentation (Ricketts, 1981) at ca. 1854 Ma (Hodgskiss et al., 2019). Proposed to be deposited within a foreland basin, the Bengal fan-type sedimentation (Ricketts, 1981) is envisioned as a consequence of the rapid exhumation of the Sugluk block at ca. 1.83 Ga (Corrigan et al., 2021). As the collision progressed, sediments of the upper Belcher Group would have filled the Hudson Bay re-entrant (Corrigan et al., 2021). These interpretations of Belcher Group sedimentation are based on regional tectonic and geophysical datasets and provide our provenance analysis study with a framework for hypothesis testing.

## 3. Materials and methods

### 3.1. Field work and sample collection

Previous mapping of the Belcher Group provided a geological and stratigraphic framework (1:125 000 scale; Jackson, 2013). Field observations for this study focused on measuring detailed bed-by-bed stratigraphic sections of the Loaf, Omarolluk, and Costello formations (Supplementary Data, Fig. S1), locations shown in Fig. 2. Samples for geochronological analysis were collected within these measured sections.

### 3.2. Mineral separation

Samples were processed for mineral separation at both the University of Saskatchewan in Canada (18CAPB007) and at Zirchron LLC in the U.S.A. (18CAPB011;18CAPB085; 19CAPB330) using standard mineral separation techniques. At the University of Saskatchewan, samples were crushed through a Terminator Jaw Crusher, pulverized using a disk mill, then sieved (90 to 300 μm) prior to water density separation. This was followed by magnetic and density separation, via a Frantz Magnetic Separator (Model L-1) with a 20-degree forward slope, voltage at 29.4 V, current at 0.45 A and methylene iodide (3.32 g/cm$^3$), respectively. At the Zirchron lab, samples (18CAPB011, 18CAPB085, and 19CAPB330) were crushed using an electrical pulse disaggregator. Minerals were separated via methylene iodide prior to magnetic separation via a Frantz Magnetic Separator, using a series of increasing amplitudes (0.4 to > 1.0 A), at which point the zircon grains were then collected as the non-magnetic component (>1.0 A). Zircon picking and mounting was conducted at the University of Saskatchewan. To decrease sample bias, a variety of representative zircon grain populations were picked, with respect to morphology, color, magnetic fractions, and grain size.

### 3.3. Backscatter electron imaging

At the Saskatchewan Research Council Advanced Microanalysis Centre in Saskatoon, Canada, polished zircon grain mounts were coated with 10 nm of high-purity Au prior to imaging using a backscatter electron detector with a 25 kV beam on a Zeiss EVO MA15 scanning electron microscope. Zircon spot targets were chosen based on the backscattered electron images, avoiding inclusions or alteration zones.

### 3.4. U-Pb and Lu-Hf isotopes

The laser ablation split-stream (LASS) ICP-MS technique was used to determine the U-Pb age and Hf isotopic composition of detrital zircon grains. At Memorial University (St. John's, Canada), a Thermo-Finnigan Element XR ICP-MS was used for U-Pb isotope system, and a Thermo-Finnigan Neptune Multicollector ICP-MS was used for the Lu-Hf isotope system. Beam diameter was 40 μm with a 10 Hz repetition rate and a laser energy of 5 J/cm$^2$. Both samples and standards were ablated for 60 s at each spot location to measure the $^{206}Pb/^{238}U$, $^{207}Pb/^{235}U$, $^{207}Pb/^{206}Pb$, $^{176}Lu/^{177}Hf$ and $^{176}Hf/^{177}Hf$ ratios. Standard-sample bracketing was implemented; twelve unknowns were analyzed followed by measurements of each standard (Plešiovice x 2, 91500 x 2, 02123 x 1, Temora-2 x 1). The primary standard used for the U-Pb isotope system was 91,500 (Wiedenbeck et al., 1995), with Plešiovice (Sláma et al., 2008), 02,123 (Ketchum et al., 2001), and Temora-2 (Black et al., 2004) as secondary standards used for quality control. The primary standard for the Lu-Hf isotope system is Plešiovice with a $^{176}Hf/^{177}Hf$ reference value of 0.282482 ± 0.000013 (2SD) (Sláma et al., 2008). All the data were normalized to Plešiovice after the mass interference and fractionation corrections were applied. Secondary standards used for quality control purposes were: 91,500 with a reference $^{176}Hf/^{177}Hf$ value of 0.282306 ± 8 (2SD) and Temora with a $^{176}Hf/^{177}Hf$ reference value of 0.282686 ± 8 (2SD) (Woodhead and Hergt, 2005). Synthetic zircon grains, MUNZirc 1 and MUNZirc 4 with a shared $^{176}Hf/^{177}Hf$ reference value of 0.282140 ± 0.00034 (2SD) (Fisher et al., 2011) were used for initial setup and beam stabilization. Isotopic ratios are reported within 2 standard error. Iolite was used for data reduction and to ensure the Lu-Hf and U-Pb signals were aligned. Hafnium is expressed as a ratio (εHf) and was calculated using the equation in Kinny and Mass (2003).

All U-Pb detrital zircon ages were filtered to include those with less than ± 10 % discordance. The youngest detrital zircon age calculation was determined via a weighted average of the three youngest detrital grains and is interpreted as the maximum depositional age for that sample. Filtering criteria (discordance ± 10 %, Th/U > 0.1, error correlation < 1) in addition to a visual inspection of zircon quality and considerations of metamorphic age were used to determine the youngest detrital grains. Metamorphic grains younger than the depositional age are not anticipated due the very low metamorphic grade.

### 3.5. Database and paleographic reconstructions

Published zircon U-Pb, zircon εHf and whole-rock εNd records from Dateview (Eglington, 2004) and other sources (including Meek et al. 2020; Puetz et al., 2024) were used to compare with clusters of detrital zircon grain U-Pb ages and εHf values from the Belcher Group samples. The εNd values were converted to εHf values using the Terrestrial Array equation of Vervoort et al. (2011) (εHf = 1.55 x εNd + 1.21) and are marked with an asterisk in the following text (εHf*). High probability regions were determined by evaluating all possible source regions for each individual grain measured in this study. For every grain analyzed, any literature sample with a crystallization age within a ± 10-million-year range and εHf value within ± 1 epsilon unit was considered to represent a potential source for that specific grain. Visualisation of the potential source locations is shown through paleogeographic reconstructions via GPlates at ca. 2015 Ma and 1850 Ma. These snapshots were selected to simulate craton positions during the deposition of the lower Belcher Group (e.g., Kasegalik Formation, ca. 2015 Ma) and upper Belcher Group (e.g., Omarolluk and Loaf formations, ca. 1850 Ma), respectively.

## 4. Results

### 4.1. U-Pb geochronology

Four samples (511 detrital zircon grains) were analyzed for U-Pb isotopes (at the same time as Hf isotopes) to constrain the maximum depositional age, detrital grain age distributions, and sedimentary provenance of the Costello, Omarolluk, and Loaf formations from the Belcher Group. Overall, backscattered electron imaging shows a lack of high U overgrowths, which is consistent with low grade (prehnite/pumpellyite facies) metamorphism. The U-Pb detrital zircon ages from the Belcher Group are shown in a combined frequency histogram with probability density curves (Fig. 4). Table 1 summarizes the detrital zircon U-Pb geochronological results including the maximum depositional age, dominant age peaks, and the range of εHf values for each sample; ages are reported with 2σ errors. Full U-Pb data results are listed in Supplementary Data (Table S1).

#### 4.1.1. Costello formation

Sample 18CAPB085 is a white to tan colored, massive quartz arenite located ~ 106 m above the contact with the Mavor Formation (Fig. 2). The six-meter-thick quartz arenite bed is bounded by laminated cross-bedded coarse-grained immature sandstone. Zircon grains are dominantly poorly- to fairly- rounded (using classification scheme of Gärtner et al., 2013) and demonstrate short and stalky length to width ratios (Supplementary Data, Fig. S2). Most zircon grains exhibit oscillatory zoning and very little to no evidence of recrystallization. One-hundred-seven detrital zircon grains were selected for LASS-ICP-MS analysis, of which 93 grains are within ± 10 % discordance. The three youngest grains (039: 2655 ± 40 Ma, 090: 2657 ± 40 Ma, and 133: 2682 ± 38 Ma) were selected for the youngest detrital zircon determination using a weighted mean, yielding a $^{207}Pb/^{206}Pb$ age of 2664 ± 22 Ma (2se). Age distribution of the concordant grains indicates a dominant grain age between 2788 and 2678 Ma with a peak at 2730 Ma (Fig. 4). The sample population is also shows smaller grain age peaks at 2889 and 3004 Ma with the oldest grain ages at 3342, 3500, and 3630 Ma.

#### 4.1.2. Lower Omarolluk Formation

Sample 19CAPB330 is a dark grey to black fine-grained sandstone in the lower member of the Omarolluk Formation ~ 700 m above the contact with the Flaherty Formation on Gilmour Peninsula (Fig. 2). Detrital zircon grains appear dominantly as short and stalky with only a small subset having longer grain morphology. The grains are fairly-rounded and display oscillatory zoning. One-hundred-thirty-five detrital zircon grains were analyzed, of which 105 are within ± 10 % discordance and have a Th/U ratio > 0.1, thus were used in assessing the detrital grain population. The three youngest detrital zircon grains (126: 1845 ± 34 Ma; 181: 1853 ± 54 Ma; and 119: 1856 ± 41 Ma) yield a weighted mean $^{207}Pb/^{206}Pb$ age of 1849 ± 24 Ma (2se). Age distribution of the concordant grains yields a broad peak age range of 1999 to 1842 Ma with the most dominant age at 1902 Ma (Fig. 4) and a smaller secondary peak at 2730 Ma.

#### 4.1.3. Upper Omarolluk Formation

Sample 18CAPB011 is dark grey to black fine-grained sandstone in the upper member of the Omarolluk Formation, from Twin Cairns Island

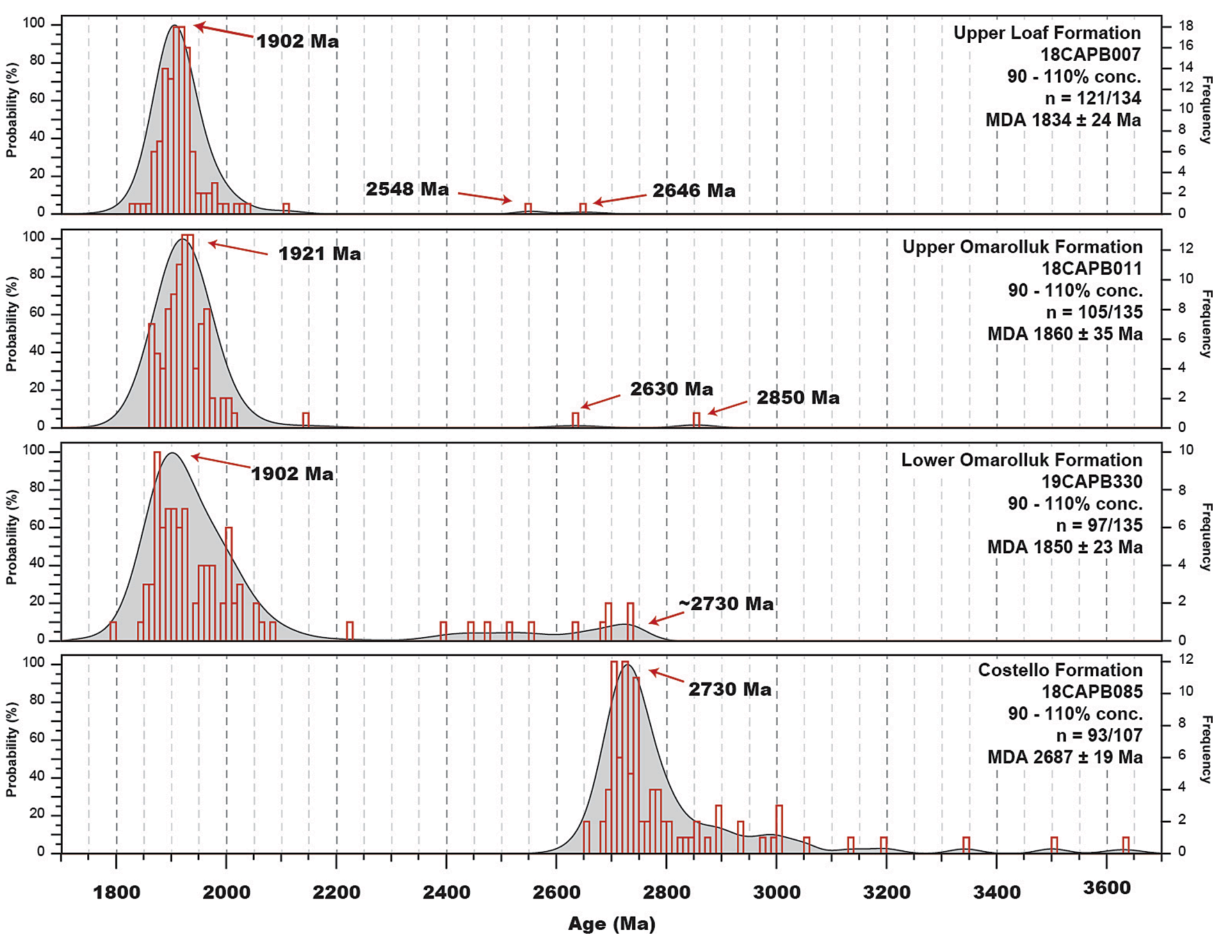


**Fig. 4.** Normalized probability distribution curves and histograms showing U-Pb detrital zircon grain age distributions for the Belcher Group formations measured in this study. Bin width set at 20 million-years. Grain age distributions of the Omarolluk and Loaf formations are centered around 1910 Ma versus the peak age of the Costello Formation at 2730 Ma, indicating a change in the source regions of their sediment supply.

**Table 1**
Summary of detrital zircon U-Pb geochronological results including the maximum depositional, dominant age peak range, and εHf range for the Costello, Omarolluk, and Loaf formations of the Belcher Group.

| Formation | Sample ID | Sample Coordinates | | Maximum depositional age[1] | Dominant age peaks[2] | εHf(t)[3] | |
|---|---|---|---|---|---|---|---|
| | | Latitude | Longitude | | | min | max |
| Loaf | 18CAPB007 | 56.67716 | −78.80824 | 1834 ± 24 Ma | 1952—1856 Ma | −5.8 | 12.1 |
| Omarolluk | 18CAPB011 | 56.52324 | −78.80432 | 1861 ± 22 Ma | 1984—1859 Ma | −4.3 | 12.2 |
| | 19CAPB330 | 56.28869 | −78.94176 | 1850 ± 23 Ma | 1999—1842 Ma | −5.8 | 15.3 |
| Costello | 18CAPB085 | 56.53241 | −79.162257 | 2664 ± 23 Ma | 2788—2678 Ma | −14.4 | 3.9 |

[1] The maximum depositional age is calculated based on the weighted mean of youngest three detrital grains for the unit.
[2] Age peaks represent any age with a greater than 50% probability.
[3] εHf calculated at time t, where t is the measured $^{207}Pb/^{206}Pb$ age. Values represent minimum and maximum values for the entire detrital zircon population of the sample.

(Fig. 2). Overall, zircon grain morphology is long, prismatic, and subrounded. Zircon grains display oscillatory zoning as well as fracturing. A total of 134 detrital zircon grains were selected yielding 135 analyses of which 102 are within ± 10 % discordance and have a Th/U ratio > 0.1. The three youngest detrital zircon grains (009: 1861 ± 38 Ma, 031: 1861 ± 35 Ma, and 064: 1863 ± 39 Ma) yield a weighted mean $^{207}Pb/^{206}Pb$ age of 1861 ± 21 Ma (2se). Age distribution of the concordant grains indicates a dominant range between 1984 and 1859 Ma with a peak age at 1921 Ma (Fig. 4). Two Archean peaks are present at 2630 and 2850 Ma.

#### 4.1.4. *Loaf Formation*

Sample 18CAPB007 is a grey-green medium to coarse grained sandstone hosted within the lower half of the upper Loaf Formation, approximately 30 m above the contact with the lower Loaf Formation on Loaf Island (Fig. 2). Zircon grains display dominantly short and long morphologies, are largely rounded, and display oscillatory zoning. One-hundred-thirty-three grains were analyzed for U-Pb yielding 134 analyses of which 119 are within ± 10 % discordance and have a Th/U ratio > 0.1. Determination of the youngest detrital zircon age using the three youngest detrital zircon grains (115: 1827 ± 54 Ma; 149: 1832 ± 32 Ma; and 045: 1845 ± 48 Ma) yields a weighted mean $^{207}Pb/^{206}Pb$ age of 1834 ± 24 Ma (2se). Age distribution of the concordant grains yields a peak age range between 1952 and 1856 Ma with a dominant grain age of 1902 Ma (Fig. 4).

### 4.2. *Lu-Hf isotopes*

All samples (n = 511 spots) were analyzed for Lu-Hf isotopes during coupled LASS-ICP-MS analysis and are plotted against U-Pb crystallization ages (Fig. 5). The εHf and $^{207}Pb/^{206}Pb$ ages are reported within 2 sigma error. The εHf values presented below are from zircon grains within ± 10 % discordance in their U-Pb age, Th/U ratios > 0.1, and exceeded a minimum analysis time of 15 s. Full Lu-Hf data results are listed in Supplementary Data (Table S1).

#### 4.2.1. *Costello Formation*

Sample 18CAPB085 contains only Archean zircon grains and yields εHf values ranging between −14.4 and + 3.9. The values are dominantly negative (79 %; n = 72/99), with the largest cluster associated with $^{207}Pb/^{206}Pb$ ages around ~ 2700 Ma (Fig. 5). For zircon grains within the peak grain age population, εHf values range between −9.9 and + 3.2 (n = 64).

#### 4.2.2. *Omarolluk Formation*

For sample 19CAPB330, Hf isotope values of the entire zircon population yield εHf values between −5.8 and + 15.3 and are dominantly positive (85 %; n = 67/79). The dominant zircon population yields εHf values between −5.8 and + 11.2 (n = 53). Sample 19CAPB330 contains a small number of Archean grains with εHf values of −0.15 at 2515 Ma; +2.3 at 2554 Ma; +6.2 and + 0.43 at 2683 and 2697 Ma, respectively; as

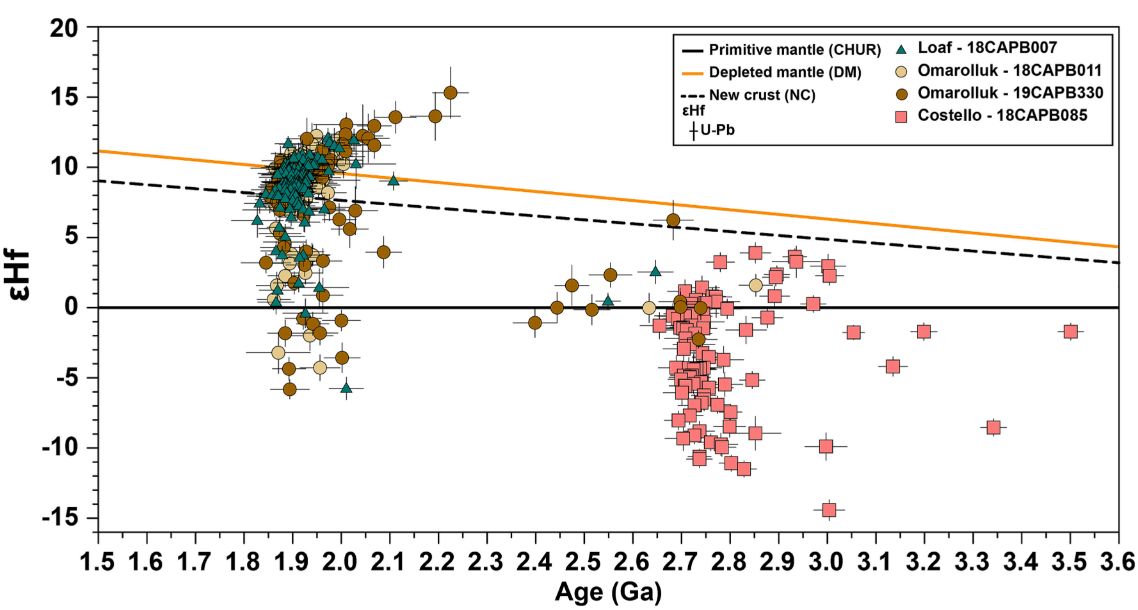


**Fig. 5.** Zircon Hf isotope data for the Loaf, Omarolluk, and Costello formations of the Belcher Group. Detrital zircon grains of the Loaf and Omarolluk formations yield dominantly positive εHf values in their youngest grain age populations but also show a large array of εHf values. The Costello Formation shows almost entirely negative zircon εHf values, all of which are Archean. Evolution lines are shown for CHUR (chondritic uniform Reservoir; Bouvier et al., 2008), DM (depleted mantle; Andersson et al., 2011), and NC (new crust: Dhuime et al., 2011). Errors shown for εHf and U-Pb ages are ± 2 sigma.

well as −2.3 at 2735 and −0.02 at 2739 Ma (Fig. 5).

For sample 18CAPB011, Hf isotope signatures of the entire zircon population yield εHf values between −4.3 and + 12.3 and are dominantly positive (96 %; n = 84/88). The dominant zircon population yields εHf values between −4.3 and + 12.7 (n = 81). While this sample is dominated by a single grain age peak centered at 1902 Ma, it also contains Archean grains with εHf values of −0.02 at 2633 Ma and + 1.6 at 2853 Ma (Fig. 5).

### 4.2.3. Loaf Formation

For sample 18CAPB007, Hf isotope signatures of the entire zircon population yield εHf values between −5.8 to + 12.1 and are dominantly positive (98 %; 117/119). The dominant zircon population yields εHf values between −0.4 and + 11.7 (n = 102). Of the few Archean grains present, their εHf values include + 0.46 for a 2548 Ma grain, and + 2.5 for a 2646 Ma grain (Fig. 5).

## 5. Discussion

In our study, we set out to test the hypothesis that sedimentary sources of the lower and middle Belcher Group were dominantly from the Superior craton (Hodgskiss et al. 2019), and that the provenance of the upper Belcher Group could be traced solely to the Sugluk block (Corrigan et al. 2021), or some combination that also included the Hudson Bay protocontinent (Jackson 2013). First, we address the age, provenance, and tectonic setting of the lower and middle Belcher Group and then that of the upper Belcher Group. The upper Belcher Group is particularly important to understand the paleogeography and paleotopography within and surrounding the Manikewan Ocean, including the Ungava and Manitoba promontories of the Superior craton. We show the entirety of available zircon U-Pb age spectra spanning most of the Belcher Group (Fig. 7), including new data from this study and existing data published by Hodgskiss et al. (2019) and Corrigan et al. (2021) to demonstrate variation in sources through the evolution of the Belcher basin.

### 5.1. Visualization of tectonic environment

Detrital zircon ages provide a unique tool that enables the visualization and comparison of sample populations to one another so as to constrain tectonic environments (e.g., Cawood et al., 2012; Barham et al., 2022). The extent of magmatic activity can vary greatly between tectonic environments and the volume of zircon production is a direct reflection of the differences in tectonic processes (e.g., Busby and Azor, 2011). Extensional settings are characterized by little to no magmatic activity and the depositional basins that form in these settings are characterized by detrital zircon populations with ages much older than the depositional age (Cawood et al., 2012). Conversely, depositional basins formed in convergent or collisional settings are characterized by detrital zircon ages much closer to that of the magmatic activity occurring at these settings. Plotting the difference between the depositional age of the unit and the age of the youngest zircon grain population (lag-time), basic tectonic setting for that basin can be inferred (Cawood et al. 2012). While this approach is valuable, it can have limitations due to a depositional age uncertainty.

Cumulative probability of U-Pb age profile plotted against lag-time for the Costello Formation population places the formation within an extensional tectonic setting (Fig. 6). The detrital zircon grains from the Costello Formation sample (18CAPB085) are dominated by ca. 2788 and 2678 Ma ages, which are significantly older than the depositional age of the Kasegalik Formation (ca. 2015.4 Ma; Hodgskiss et al. 2019) – the oldest unit of the Belcher Group. There are no direct depositional age constraints for the Costello Formation. Given the current age framework (Fig. 3), the Costello Formation must be younger than ca. 2015 Ma and older than the ca. 1870 Ma cross-cutting Haig intrusion. Hodgskiss et al. (2019) estimated the deposition of the Mavor to Rowatt formations to

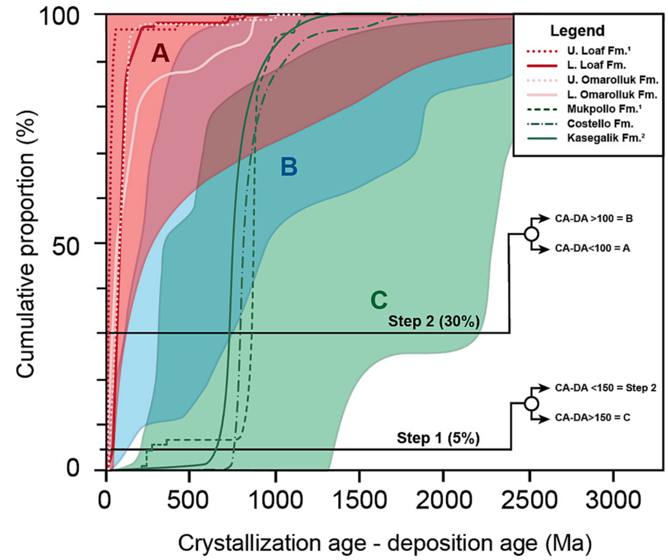


**Fig. 6.** Cumulative probability versus lag time (Ma) for detrital zircon grains of the Loaf, Omarolluk, and Costello formations, along with published detrital zircon grains from the upper Loaf and Mukpollo formations (Corrigan et al., 2021) and the Kasegalik Formation (Hodgskiss et al., 2019). Fields are defined by geodynamic settings according to the difference between crystallization age and deposition age (lag time) of a detrital zircon grain population (Cawood et al., 2012). Field A (red) defines convergent settings, field B (blue) defines collisional settings, and field C (green) defines extensional settings. The upper and lower/middle Belcher Group formations plot in different tectonic setting fields, reflecting a change in geodynamic setting of the Belcher basin from extensional/passive margin sedimentation to a convergent setting during the closing of the Manikewan Ocean. (For interpretation of the references to color in this figure legend, the reader is referred to the web version of this article.)

have occurred between 1940 and 1880 Ma. With a stratigraphic thickness of ~ 940 m, we calculate a sediment accumulation rate of 0.016 mm/yr over 60 million years, which places deposition of the Costello Formation ca. 1930 Ma. Using a depositional age of 1930 Ma, the average time between zircon grain crystallization and deposition is 875 million-years (Fig. 6). Following the parameters of Cawood et al. (2012), if the youngest 5 % of grains have a lag time greater than 150 million-years the formation falls within the extensional setting field (Fig. 6).

Deposition of the Omarolluk Formation commenced at ca. 1854 Ma (Hodgskiss et al., 2019) but its overall duration is poorly constrained. Using 1854 Ma as a conservative approximation for the depositional age of both Omarolluk Formation samples (19CAPB330 and 18CAPB011), the youngest 30 % of grains have a lag-time of less than 100 million-years, placing both samples within the convergent setting field (Fig. 6). A similar lag-time of about 90 million-years characterizes the Loaf Formation, assuming a depositional age of 1835 Ma, placing the unit within the convergent setting field (Fig. 6). Circa 1835 Ma, however, represents only a *maximum* age constraint on deposition and cannot be considered a direct proxy for true depositional age, but rather an approximation for depositional age given the lack of any additional age constraints.

### 5.2. Age and provenance of lower and middle Belcher Group

Combined histogram and probability density plots for the Kasegalik Formation indicate a dominant grain age around 2723 Ma with smaller peaks at 2667 Ma and 2834 Ma (Fig. 7). Although a single youngest grain at 2066 ± 22 Ma provides a maximum age constraint, the depositional window of the Kasegalik Formation is more accurately constrained between ca. 2018.5 Ma and 2015.4 Ma (Hodgskiss et al. 2019). The Mukpollo Formation shows a dominant grain age between 2740 and 2687 Ma with a peak age at 2713 Ma and subdominant peaks at 2990,

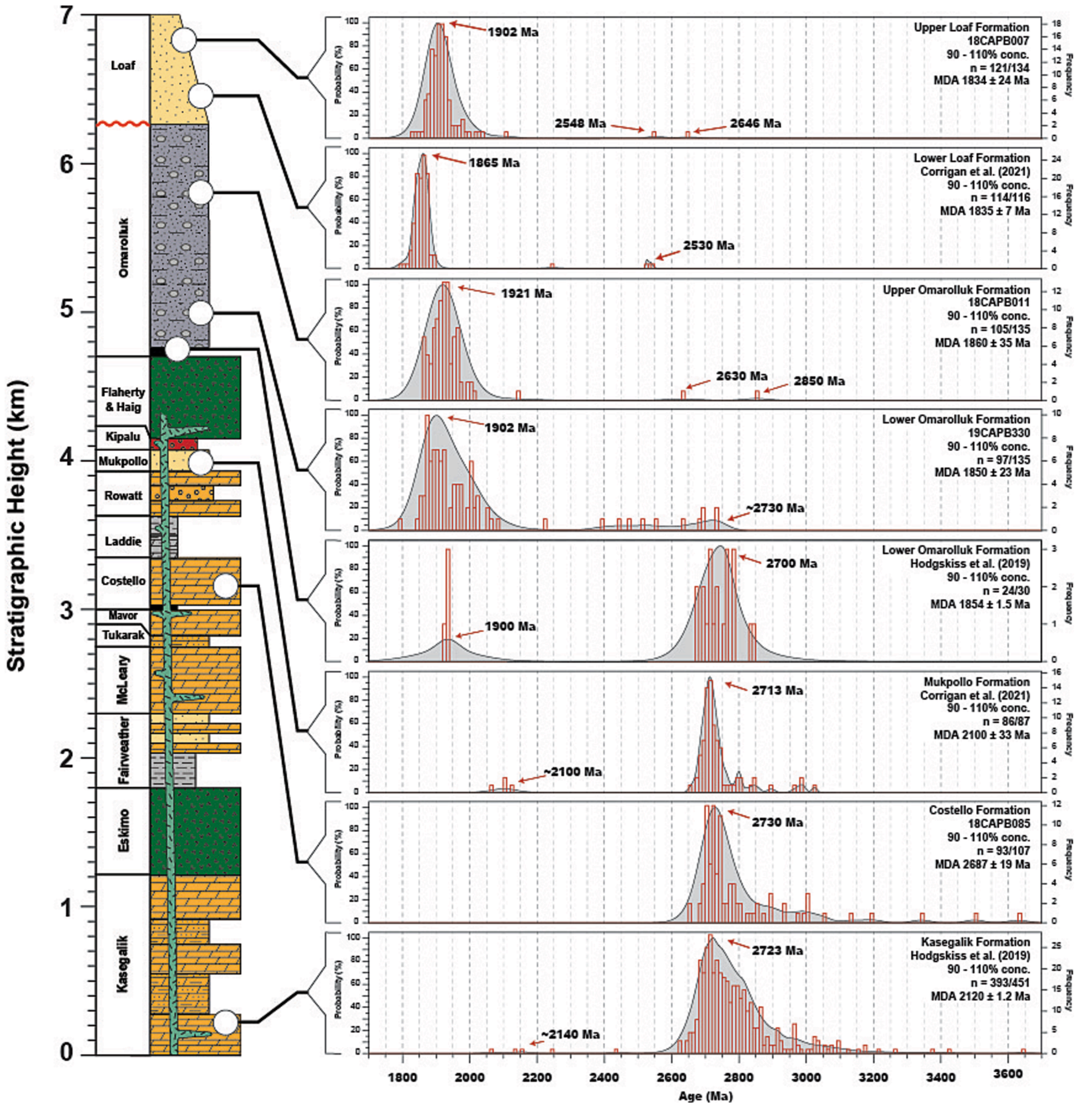


**Fig. 7.** Combined normalized probability density curves and histograms of all known detrital zircon populations from the Belcher Group demonstrating a fundamental shift in sediment source between the lower/middle and upper Belcher Group formations. Representative samples from the lower/middle Belcher Group come from the Kasegalik Formation (Hodgskiss et al. 2019), Costello Formation (this study), and the Mukpollo Formation (Corrigan et al. 2021). Representative samples from the upper Belcher Group come from the Omarolluk Formation (this study and Hodgskiss et al. 2019) and from the Loaf Formation (this study and Corrigan et al. 2021). The lower/middle Belcher Group samples show a similar grain age peak centered around 2720 Ma, indicating their sediments were likely derived from common sources. The upper Belcher Group samples record a shift to dominantly Paleoproterozoic sources, where the dominant grain population is ca. 1920 Ma in the lower Omarolluk Formation and ca. 1865 Ma in the lower Loaf Formation.

2810, and 2100 Ma (Fig. 7). The Costello Formation documents a dominant detrital zircon grain population centered at 2730 Ma and dominant age range between ca. 2788 and 2678 Ma, like the Kasegalik and Mukpollo formations (Fig. 7). Visual comparison of the grain populations of all three units indicates comparable zircon U-Pb spectra (Fig. 7). This visual comparison is bolstered by statistical comparison of the three formations using a K-S test which yields a near-zero stress value ($2.1 \times 10^{-14}$) and confirms these units share similar provenance sources (Supplementary Data, Fig. S3).

Paleo-plate reconstruction for 2015 Ma depicts the Superior craton as a singular continental mass surrounded by ocean with very few adjacent cratonic bodies (Fig. 8C). Thus, the sources for the lower Belcher Group sediments are expected to be derived entirely from the Superior craton. However, the Superior craton experienced nearly continuous magmatism between ca. 3.0 and 2.7 Ga (Davis et al., 2005; Percival, 2007), hence identifying specific source terranes within the

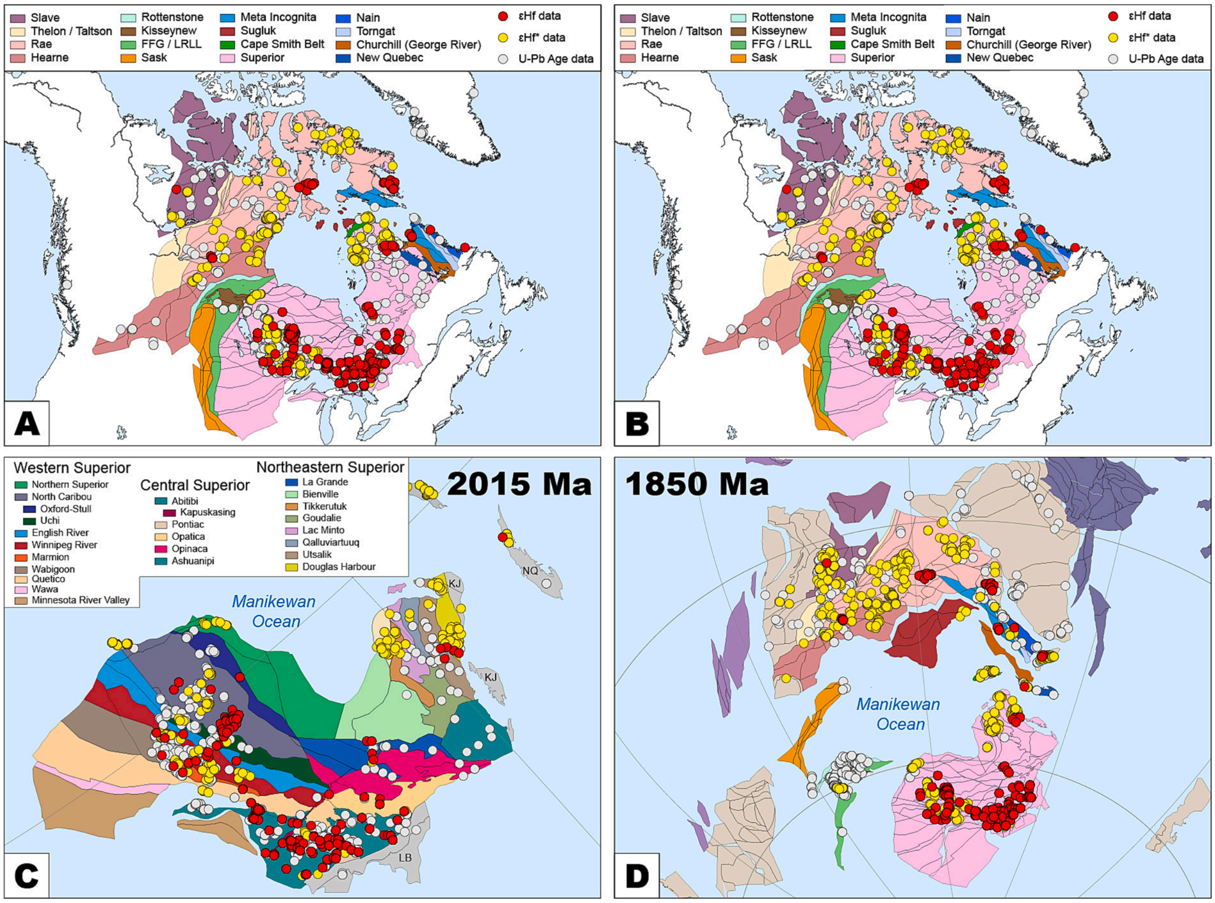


**Fig. 8.** Modern day and paleogeographic distribution of potential sediment sources for the lower and upper Belcher Group. **Panels A and B** document the location of U-Pb potential source rock ages (grey circles) that fall within the peak grain age ranges for the two groups. The red circles denote the location of εHf data while yellow denotes εHf* data of samples within 10 million years and 1 epsilon unit of individual zircon grains measured from the Belcher Group. **Panels C and D** depict the paleogeographic orientation of the cratons during deposition of the lower and middle Belcher Group (C) at 2015 Ma and the upper Belcher Group (D) at 1850 Ma. Although the Costello Formation was likely deposited at ca. 1930 Ma, the configuration of the Superior craton was relatively static over this interval, remaining isolated without any collisional or accretionary additions to its margins. (For interpretation of the references to color in this figure legend, the reader is referred to the web version of this article.)

larger Superior craton presents a challenge. Thus, the εHf and εHf* records represent a useful tool to decipher terrane provenance within the Superior craton.

Comparison of zircon grain populations suggests a gradual change in sediment sources across the depositional period of the lower and middle Belcher Group. Older grains between ca. 2840 and 2680 Ma within the Costello Formation are explained by several terranes from the west, south and northeastern parts of the Superior craton (Fig. 8C; Supplementary Data, Table S2), while grains between 2680 and 2600 Ma are found within the western and southern regions of the Superior craton (Supplementary Data, Table S2).

Potential candidate sources with western Superior craton such as the Marmion terrane document magmatic activity between ca. 3000 and 2690 Ma with major pulses at 3000, 2960, 2930, and 2890 Ma (Bjorkman, 2017). Reported εHf values from the region range from + 1.2 to + 2.8 for ages between ca. 2957 and 3000 Ma (Davis et al., 2005) while values from the Winnipeg River sub-province range from −5.3 to −2.6 for ages between ca. 3225 and 3050 Ma (Davis et al., 2005). Both terranes show good overlap with the lower-middle Belcher Group samples between the ages of 2890 and 3250 Ma, but document more juvenile signatures for ages corresponding with the peak grain age at 2720 Ma. Li et al. (2020) measured similarly juvenile εHf signatures for the North Caribou terrane as well as from the Island Lake and northern Uchi domains. The North Caribou and Winnipeg River terranes are the only sources that are a match for ca. 2840 to 2600 Ma grain ages in our dataset with similar εHf values (Fig. 9B). A minor detrital zircon age population at ca. 2100 Ma is present in both the Mukpollo and Kasegalik formations (Fig. 7). This age population was attributed to either the Marathon and Biscotasing (ca. 2126 – 2101 Ma) and/or Fort Francis (ca. 2076 Ma) mafic dyke swarms in the western Superior craton (Buchan et al., 2007; Corrigan et al., 2021; Hodgskiss et al., 2019). However, neither Hf nor Nd isotope data exists for any of the dyke swarms making it difficult to corroborate these potential sources.

Igneous activity within the southern Superior craton such as in the Abitibi and surrounding regions is characterized by predominantly radiogenic εHf values for the ca. 2850 to 2680 Ma period (Boily et al., 2009; Cleven et al., 2020; Mole et al., 2021; Polat et al., 2022; Stevenson et al., 2006). While some of the detrital grains found within the lower and middle Belcher Group can be explained by sources in the southern Superior craton, isotopic values from the region are overall too juvenile to explain the remainder of the data.

Considering the overall positive εHf values for Archean rocks found within the western and southern regions of the Superior craton, it is unlikely that the Costello Formation was dominantly sourced from the south-west. Alternatively, Neoarchean plutonic rocks of the northeastern Superior craton are overall more evolved than their Mesoarchean counterparts and are candidates for the older grain populations in the sample set (Supplementary Data, Table S2). Whole-rock Nd isotope values from the Bienville domain yield εHf* values between −6.6 and 1.8 with an average of around −2.0 for rocks dated between

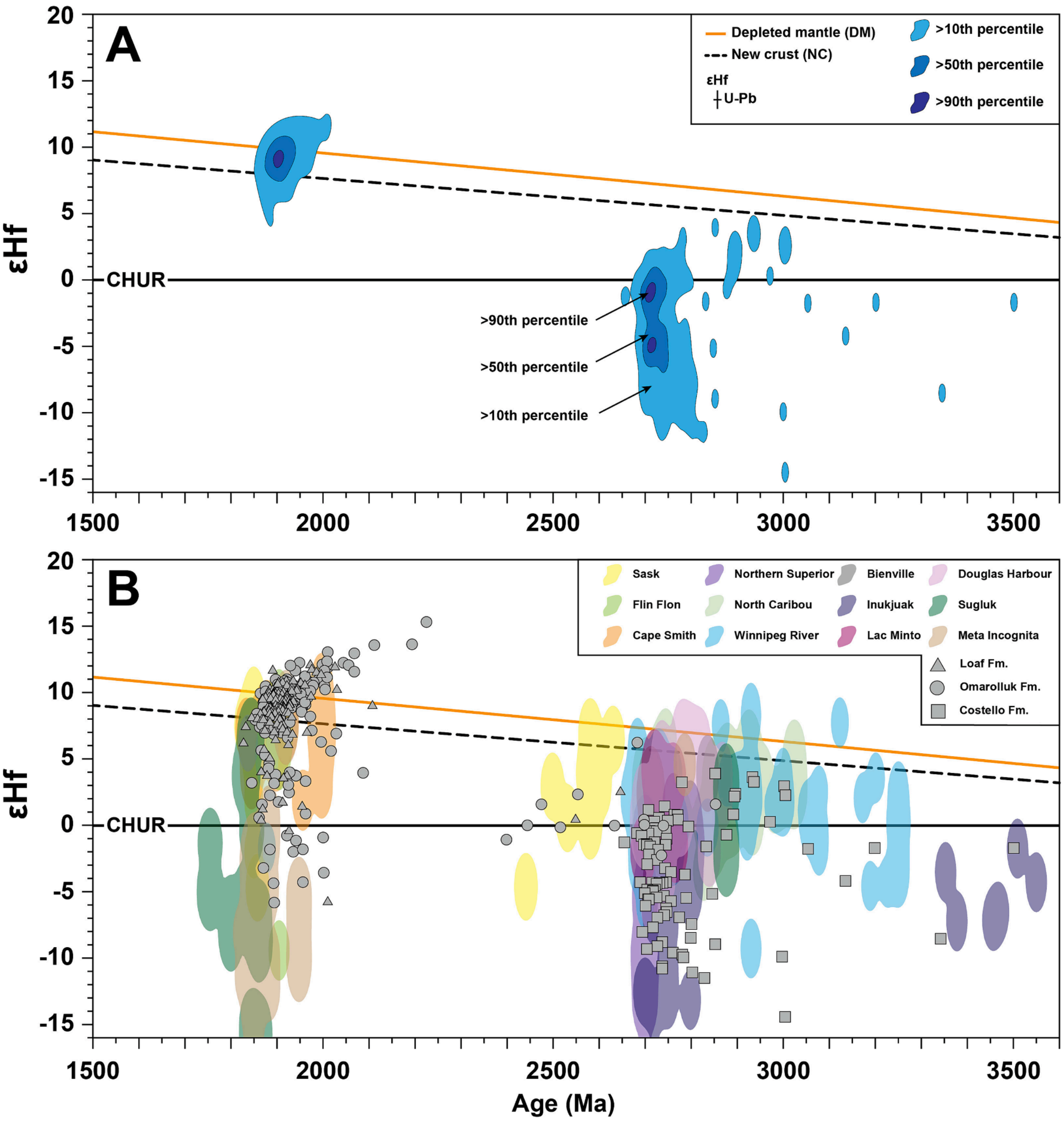


**Fig. 9.** **A**) Simplified bivariate kernel density estimation (2dKDE) of Belcher Group εHf and U-Pb zircon data showing the 10th, 50th, and 90th percentiles. Bandwidth of U-Pb is 10 million years and 1 epsilon for εHf. This shows that the highest density of εHf data for the Omarolluk and Loaf formations fall in the distribution of + 8.5 to + 10 for U-Pb ages between 1890 and 1915 Ma, whereas the highest density of εHf data for the Costello Formation fall in the distribution of −5.5 to −4.5 and −2 to 0 for U-Pb ages between 2700 and 2725 Ma. **B**) Simplified 2dKDE of combined literature εHf and εHf* values against U-Pb zircon to determine probable grain provenance. Contour interval is conservatively defined to include all data within ± 10 Myr and ± 1 epsilon unit of the original point. This shows significant overlap with juvenile volcanic units from terranes such as the Cape Smith belt and rocks from the Flin Flon-Glennie collage, as well as the Sugluk block, for the upper Belcher Group samples. Data for the lower and middle Belcher Group consistently plot within the Inukjuak, Douglas Harbour, Bienville, and Lac Minto terranes of the Superior craton.

ca. 2756 and 2690 Ma (Boiley et al. 2009). The Tikkertuk domain records εHf* values between −7.5 and + 12 and an average of −0.6 for ages between ca. 2766 and 2675 Ma (Boiley et al. 2009). Both the Bienville and Tikkertuk domains yield values consistent with those of the lower Belcher Group. We therefore conclude that Costello sediments were likely principally derived from regions located near the Belcher basin, such as the Inukjuak, Tikkertuk, Lac Minto, and Bienville domains as well as from the Douglas Harbour domain located further to the northeast (Supplementary Data, Table S2). The northeastern Superior craton accounts for the greatest proportion of the older detrital grains in the Costello Formation, while the younger grain populations between ca. 2680 and 2600 Ma are best explained by sources located in the west, such as the Winnipeg River and North Caribou terranes.

### *5.3. Age and provenance of the upper Belcher Group: Omarolluk and Loaf formations*

The < 1855 Ma Omarolluk and < 1835 Ma Loaf formations contain detrital zircon grain populations that are significantly younger than those found in the formations that define the lower and middle Belcher Group (Fig. 7). The lower member of the Omarolluk Formation contains a dominant age population between 1999 and 1842 Ma, with a peak at 1921 Ma and a minor mode around 2730 Ma (Fig. 4). The upper member of the Omarolluk Formation is characterized by a similar range from ca. 1984 to 1859 Ma but a slightly younger peak at ca. 1902 Ma (Fig. 4). The overlying upper Loaf Formation shares the same ca. 1902 Ma age mode as the upper Omarolluk sample (Fig. 4), while the zircon population from Corrigan et al. (2021) documents a younger peak at 1865 Ma (Fig. 7). Thus, while there was minor detrital input from Archean sources during the earliest stages of Omarolluk sedimentation, the sediment source changed almost entirely to Paleoproterozoic sources during deposition of the upper Omarolluk Formation which continued during deposition of the Loaf Formation. A paucity of Archean U-Pb ages in the upper Belcher Group signals an abrupt transition away from the older sources of Superior craton as the dominant sediment source (Supplementary Data, Table S3). While the detrital record indicates a shift away from Superior sources it also highlights the differences between the Omarolluk and Loaf grain populations. As such, we analyze the provenance of the upper Belcher Group by separating the two formations, because their presumed depositional ages are nearly 20-million-years apart. Also, we suggest that the shift in their depositional environments is a major indicator of changing provenance due to fundamental changes in the tectonic architecture of proto-Laurentia between the two time frames, which resulted in an increased proximity of potential source terranes (Fig. 8D).

First, we consider candidate sources from the peripheries of the Superior craton that can explain the detrital grain population of the Omarolluk Formation (Fig. 8D). Rocks from the western Reindeer zone, such as those of the Flin Flon–Glennie and La Ronge–Lynn Lake collage are viable candidates because they document volcanic and intrusive igneous activity between ca. 1920 and 1860 Ma during the closure of the Manikewan Ocean that continued to a lesser extent until terminal collision ca. 1810 Ma (Corrigan et al. 2009). Volcanic arc rocks of the Flin Flon–Glennie domain are consistent with juvenile magma production yielding εHf* values between + 4.7 and + 9.6 at 1900 Ma (Stern et al., 1995) and felsic to intermediate plutonic rocks associated with younger arc evolution yield εHf* values between + 4.5 and + 8.5 at ca. 1875 – 1890 Ma (Whalen et al., 1999, 2016). When compared to the upper Belcher Group, there is significant overlap between these εHf* values and the measured εHf values from this study (Fig. 9B and Supplementary Data, Table S3), thus we interpret that a subset of the detrital grains found within the Omarolluk Formation samples was derived from the western Reindeer zone. This is consistent with the timing of formation of the Flin Flon-Glennie crustal block ca. 1870 (Lewry, 1990; Lucas et al., 1996). The resulting amalgamation of the Flin Flon-Glennie block resulted in a series of thrust-stacked assemblages overtop rocks of the underplating Sask craton (Ashton et al., 2005). A major sedimentation event ca. 1855 to 1830 Ma occurred in this collage as well as on the Kisseynew domain with the deposition of the Missi Supracrustal Suite and the Burntwood Group (Ansdell et al., 1995; Zwanzig et al., 1990). Importantly, this overlaps with the timing of the deposition of the upper Belcher Group. Additionally, our dataset includes several grains with U-Pb ages around 2500 Ma (Fig. 5), which are consistent with Archean basement ages for the Sask craton between 2550 and 2420 Ma (Ashton et al., 2005, 1999; Chiarenzelli et al., 1998; Corrigan et al., 2007; Rayner et al., 2005). Corresponding εHf data for the samples in our dataset yield values between −0.15 and + 2.3 (Fig. 6) which are also consistent with values reported in the Sask craton (Bickford et al., 2005; Rayner et al., 2005) and form the basis of our interpretation of the Sask craton as a source. Another possibility to explain ca. 2520 Ma grains is the Partridge Breast block, which may

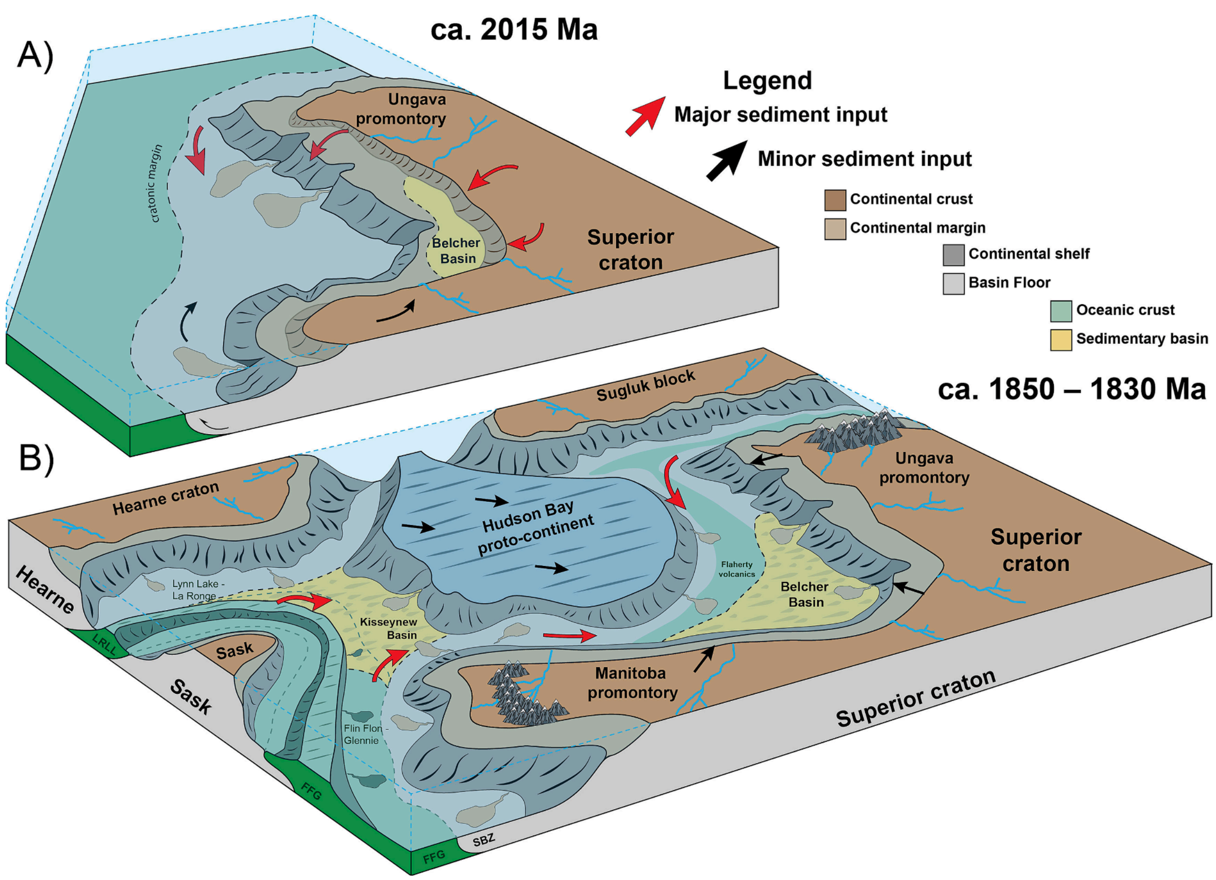


**Fig. 10.** Paleo-basin reconstruction at ca. 2015 (A) and 1850 Ma (B) displaying the main phases of sedimentation within the Belcher basin. Panel A) depicts the Superior craton as an isolated continent during deposition of the lower and middle Belcher Group. Provenance analysis of lower and middle Belcher Group sediments indicate the basin principally received detrital input from Archean domains of the Superior craton. Panel B) depicts the envisaged orientation of the Superior craton with respect to surrounding cratons and terranes during deposition of the Omarolluk Formation ca. 1850 Ma. Our provenance analysis shows that sediments were derived from several sources along an arcuate path including the western Reindeer zone and the Manitoba and Ungava promontories of the Superior craton. Arrows depict the general region from which sediments were derived. LRLL: La Ronge-Lynn Lake; FFG: Flin Flon-Glennie, SBZ: Superior Boundary Zone.

have been exposed during terrane accretion ca. 1865 to 1830 Ma and has εHf* values of + 2.0 and + 2.3 (Martins et al., 2022).

A potential basin-adjacent source of the upper Belcher Group detritus could be the Hudson Bay proto-continent (Fig. 10B). The Hudson Bay proto-continent is an aeromagnetic anomaly located in the center of the bay interpreted to represent a cratonic mantle keel of a smaller Archean continent, that is not exposed at surface (Roksandic, 1987; Eaton and Darbyshire, 2010). It is interpreted to potentially contain ca. 1.89–1.87 Ga magmatism based on a tectonic interpretation of the region, where it was the upper plate during collision with the Hearne craton (Pehrsson et al., 2013). In this scenario, we envision that uplifted material was eroded and shed into the Belcher basin during the deposition of the Omarolluk Formation after ca. 1855 Ma. However, the lack of exposure makes this idea difficult to test.

Looking to candidate sources from the north-eastern periphery of the Superior craton, the Cape Smith fold belt and Narsajuaq arc (Sugluk block) host a number of possible ca. 1960 and 1835 Ma source candidates (Dunphy and Ludden, 1998; Hegner and Bevier, 1991; Smith and Ludden, 1989). Whole-rock Nd isotope data along with U-Pb ages from the Chukotat Group (Smith and Ludden, 1989) of the Cape Smith fold belt yield εHf* values between + 7.3 and + 8.2 for rocks dated between 1880 and 1920 Ma. Intrusive rocks from the 1860 to 1845 Ma Cape Smith suite yield εHf* values between + 3.5 and + 5.6. Similar values are reported from the Narsajuaq arc, which records εHf* values between + 6.2 and + 7.4 for the ca. 1863 to 1844 Ma Gneissic Suite and + 3.8 to + 7.4 for the ca. 1835 Ma Younger Suite (Dunphy and Ludden, 1998a). Both the Cape Smith fold belt rocks and intrusions, as well as the Narsajuaq arc intrusions yield εHf* consistent with the younger grain populations within both the upper Omarolluk and the Loaf formation (Supplementary Data, Table S3). However, the intrusions of the Narsajuaq arc are largely too young to account for the peak grain ages measured in our upper Belcher Group samples (Fig. 9B). That said, basement orthogneisses (ca. 2980 to 2781 Ma) and ca. 2550 Ma granitic rocks of the Sugluk block host could account for the Archean populations (Corrigan et al., 2021). Possible sources situated around the Sugluk block, such as Meta Incognita and the Aasiaat domain document magmatic activity during the peak grain age windows for both upper Belcher Group formations but yield εHf* and εHf values that are too evolved to account for the values measured in this study (Supplementary Data, Table S3).

Within the interior of the Superior craton, candidate sources are limited for both the Omarolluk and Loaf formations. The Omarolluk Formation detrital population contains only a few grains with ages greater than 2600 Ma (n = 7/199). Of those grains, terranes within the western Superior craton (i.e., Northern Superior, North Caribou, Marmion, Oxford-Stull, and Winnipeg River) are the most likely sources, however, regions in the northeastern part of the craton (i.e., Tikkertuk, Inukjuak and Douglas Harbour) are also possible candidates (Supplementary Data, Table S3). In addition to the Archean sources, the Omarolluk Formation contains grains between 1880 and 1860 Ma with εHf values between + 0.96 and + 1.74, which are consistent with values from both the Molson dykes and Winnipegosis belt (Ciborowski et al., 2017).

### 5.4. Tectonic implications of the Belcher Group provenance

Paleogeographic reconstructions at 2015 Ma indicate the Superior craton was isolated from other continents and was forming laterally extensive passive margin sequences following rifting of its continental margins (Fig. 9C). Our provenance analysis shows that early in its history, the Belcher basin principally sourced sediments from the north-eastern Superior craton (e.g., Lac Minto, Utsalik, and Douglas Harbour domains) and to a lesser extent from the south-west Superior craton (e.g., North Caribou and Winnipeg River terranes). Regions constituting the basin margins such as those directly adjacent to the present-day location of the Belcher Group (i.e., Inukjuak, Tikkertuk, and Bienville domain) may have also been a significant source of detrital material (Fig. 10A). Detrital zircon populations with ages spanning approximately 100 million yr. across the Kasegalik, Costello, and Mukpollo formations yield similar detrital age spectra, with only minor variations in the presence or absence of the youngest (ca. 2100 Ma) and oldest (ca. 3000 to 3600 Ma) populations (Fig. 7). Thus, their sources were largely consistent over the depositional period of the lower and middle Belcher Group sediments (2018 to > 1870 Ma), indicating an overall quiescent and unchanging tectonic setting for the lower and middle Belcher Group.

A major change in the Belcher basin occurred ca. 1870 Ma with the emplacement of the volcanic flows of the Flaherty Formation, which was also associated with a reversal in paleoslope of the basin that changed it from ocean basin-facing to craton-facing (paleoflow towards the present-day east). The specific tectonic setting represented by the Flaherty volcanism is not well established, but previous studies agree its geochemical signatures are consistent with rifting, or perhaps local extension within an overall compressional tectonic setting (Baragar, 2007; Chauvel et al., 1987; Legault et al., 1994; Ricketts et al., 1982), or as part of a mantle plume of the Circum-Superior large igneous province (Ciborowski et al., 2017; Ernst and Buchan, 2004). The Flaherty Formation has E-MORB characteristics and cross-plots of Th/Yb versus Nb/Yb demonstrate an increase in Th/Yb (Supplementary Data, Fig. S4) consistent with crustal contamination (Pearce 2008). Cross-plots of Ti/Yb versus Nb/Yb indicate the Flaherty Formation has a MORB affinity with evidence of plume interaction (Supplementary Data, Fig. S4), thus ruling out a volcanic arc interpretation.

Terminal continent–continent collision of the Himalayan-scale Trans-Hudson orogen occurred between ca. 1830 and 1790 Ma (Corrigan et al., 2021, 2009; Hoffman, 1990; Weller and St-Onge, 2017). A voluminous sedimentary record would have also been produced in *syn*-orogenic basins due to the erosion of mountain belts formed from the accretion of magmatic arcs and microcontinental blocks, such as the Cape Smith belt (ca. 1870 Ma; St-Onge et al., 2000) or Sugluk block (ca. 1830 Ma; Corrigan et al., 2021) onto the Superior craton margin or the formation of the Superior Boundary Zone (ca. < 1860 Ma; White et al., 2002). The timing of deposition of the Omarolluk and Loaf formations from ca. 1855 to at least ca. 1835 Ma suggests their fill could be *syn*-orogenic. Indeed, the traditional interpretation of the Omarolluk Formation is that it represents *syn*-orogenic flysch deposition by turbidity currents while the Loaf Formation is associated with fluvial to shallow marine distal molasse deposited within a foreland basin (Jackson, 2013; Ricketts, 1979, 1981). Paleocurrent data from flute cast structures in the Omarolluk Formation show that flow was predominantly toward the southeast during the deposition of the Omarolluk Formation, while trough cross-bedding in the Loaf Formation shows paleoflow azimuths dominantly to the south and southeast (Ricketts 1979; 1981; Ricketts and Donaldson 1981), suggesting sources mostly from the northwest of the present-day Belcher Islands during Omarolluk-time and mostly from the north during Loaf-time.

Corrigan et al. (2021) proposed the collision of the Sugluk block and the Superior craton at the Ungava Promontory as the main source of detritus that led to the foreland basin fill. Southward thrusting along the Bergeron suture ca. 1870 Ma is thought to have been responsible for the obduction of the Watts Group ophiolite as well as the Parent/Spartan Group (St-Onge et al., 2000). Evidence of the early obduction is present within both formations of the upper Belcher Group, as several grains from all three samples match the + 5 to + 10 spread in εHf* values reported from the ophiolite at ca. 2000 Ma (Supplementary Data, Table S3; Hegner and Bevier, 1991). Detrital input from the Cape Smith region was relatively minor during deposition of the Omarolluk Formation, however, this becomes more prominent during deposition of the Loaf Formation (Supplementary Data, Table S3). Continual southward thrusting between ca. 1870 and 1820 Ma led to the formation of the Cape Smith fold belt (Lucas, 1989). Syn-collisional eclogite-facies metamorphism associated with the collision between the Churchill province (Sugluk block) in the Cape Smith belt is constrained between ca. 1831 and 1820 Ma (Weller and St-Onge, 2017). Undoubtably, increased tectonic activity associated with the collision generated significant volumes of detritus and the timing of metamorphism overlaps with Loaf Formation deposition. We see evidence of increased delivery of detritus from the Cape Smith region within the Loaf Formation corresponding to εHf* values reported from the Chukotat Group (+7.8 to + 8.2) at 1920 and 1880 Ma (Hegner and Bevier, 1991) and from the Narsajuaq arc (+6.7 to + 7.3) at 1863 and 1835 Ma (Dunphy and Ludden, 1998).

Sediment delivery during the deposition of the Omarolluk Formation was influenced by tectonic processes operating within the Reindeer Zone and along the Superior Boundary Zone. Following the emplacement of the Flaherty volcanic flows ca. 1870 Ma, the Belcher basin was filled by sediments generated from the accretion of the Hudson Bay proto-continent and the Hearne craton between ca. 1890–1870 Ma (Pehrsson et al., 2013). The collision resulted in the westward thrusting of the Hudson Bay proto-continent onto the Hearne craton thereby shedding detritus with a Hudson Bay proto-continent affinity into the Belcher basin. Synchronous with the Hearne craton collision was the accretion and unification of the Flin Flon–Glennie domain between 1880 and 1865 Ma and emplacement of the Flaherty Formation ca. 1870 Ma within the Belcher basin and Sleeper Islands (Fig. 10B). A detrital zircon signature between 1880 and 1870 Ma and a small peak at 2550 Ma supports input of both Flin Flon-Glennie and Sask craton sources. These sediments were likely generated during thrusting of the Flin Flon-Glennie domain overtop the Sask craton after ca. 1850 Ma and transported to the Belcher basin through a series of longshore currents. Following the consolidation of the Flin Flon-Glennie domain a series of thrust stacks formed in response to the collision with the Sask craton ca. 1870 and 1843 Ma (Ashton et al., 2005). The underplating of the Sask craton, which preserves Archean basement rocks between ca. 2550 and 2420 Ma (Ashton et al., 2005, 1999; Chiarenzelli et al., 1998; Corrigan et al., 2007; Rayner et al., 2005), is the proposed mechanism responsible for generating sediments with a Sask craton-affinity found within the Belcher Group detritus, according to our interpretation.

Modern-day submarine fan sedimentation is either dominantly river-fed or fed from longshore currents (Gamberi et al., 2015) and similar processes were likely active during the Paleoproterozoic. Paleocurrents measured within the Omarolluk Formation and a thinning of its facies towards the southeast suggest transport dominantly towards the southeast (Ricketts, 1981). Thus, we envision that Omarolluk submarine fan sedimentation was sustained by a mixture of longshore currents that would be sourced from a combination of the Manitoba Superior margin and the Hudson Bay protocontinent following counterclockwise currents (as expected in the southern hemisphere) as well as from fluvial systems transporting sediments directly from parts of the continental interior (Fig. 10B).

The deposition of the Loaf Formation represents a transitional phase where western sediment sources are dominantly replaced by sources located to the north. These northern sediments are dominantly derived from terranes within the northeastern Superior craton and from the Sugluk block. The detrital grain population of the Loaf Formation samples consists of Archean grains and the additional constraint of the Hf isotopes suggests that a subset of those grains was derived from the Tikkertuk, Inukjuak, and Douglas Harbour terranes located to the present-day north of the Belcher Group on the Superior craton. The youngest grain ages within the sample set are compatible with rocks of the Cape Smith belt and those of the Narsajuaq arc (ca. 1863–1830 Ma; Supplementary Data, Table S3). Comparison of the younger dominant age peak measured by Corrigan et al. (2021) is also consistent with sources in the area. From a sediment delivery perspective, these observations accord with the depositional environment suggested for the Loaf Formation, which documents a transition from marine to fluvial deposition. Tectonically, it is also consistent with the accretion of outboard volcanic arcs beginning at 1870 Ma and ending with terminal collision between 1830 and 1790 Ma (Corrigan et al., 2009; 2021). We conclude, however, that the Sugluk block does not account for the entire detrital population present in the Loaf Formation as was previously envisioned in an orocline setting.

## 6. Conclusions

This study provides the first detrital zircon U-Pb, Hf isotope record for the Belcher Group. New coupled detrital zircon U-Pb, Hf data from three formations in the Belcher Group (Costello, Omarolluk, and Loaf formations) are used in this study in conjunction with previous detrital zircon U-Pb data from the literature (Kasegalik, Mukpollo, and Loaf formations) to determine the sedimentary provenance of the lower, middle, and upper Belcher Group. We determined maximum depositional ages for all three formations (ca. 2664 Ma for Costello, ca. 1850 Ma for Omarolluk, and ca. 1834 Ma for Loaf) that agree with previously published age data. Detrital zircon analysis along with field observations corroborate an extensional and/or passive margin setting for the lower and middle Belcher Group, and a collisional setting for the upper Belcher Group.

The lower and middle Belcher Group (Kasegalik to Mukpollo formations) is characterized by sequences of transgressive carbonate platforms built along a passive margin of the Superior craton that initiated deposition sometime prior to 2018 Ma. Detrital zircon grains from the lower and middle Belcher Group document sediment sources across the Superior craton, dominantly from the northeast as well as from the west. Analysis of individual detrital ages from the lower and middle Belcher Group reveal principally negative εHf values characteristic of Archean terranes located in the northeastern Superior craton (Fig. 9). Our results indicate sediments were primarily derived from the northeastern Superior craton and represent a mixture of sources between Inukjuak, Tikkertuk, Douglas Harbour, Lac Minto, and Bienville domains. Detrital input of the younger ca. 2720 to 2600 Ma grains is indicated to have been from western Superior sources such as the North Caribou and Winnipeg River terranes. Thus, the lower and middle Belcher Group was sourced from a wide geographic area of the Superior craton, as would be expected for a passive margin setting.

The detrital zircon record for the upper Belcher Group (Omarolluk and Loaf formations) documents a diverse range of sediment sources reflecting deposition during a magmatically and tectonically active time that encompasses the last ca. 20 to 30 million years of the closing of the Manikewan Ocean. The Loaf Formation deposition is separated from the Omarolluk Formation by at least 20 million-years based on maximum depositional age constraints, thus we assess their provenance in the context of two depositional units that we interpret are separated by an unconformity. We document juvenile detrital zircon εHf values in the Omarolluk Formation consistent with volcanic terranes located in the Flin Flon-Glennie domain and a small subset of grains with Sask craton-like ages and εHf values. We interpret the combination of these two populations as evidence of longshore currents responsible for transporting sediments along the cratonic margin of the Superior craton and into the Belcher basin. Our provenance analysis using detrital zircon U-Pb and Hf isotope data suggests that neither the Loaf nor the Omarolluk Formation were solely sourced from the Sugluk block. The Omarolluk Formation was likely derived from a range of locations that define an arcuate path from the Reindeer zone and Manitoba promontory to the Ungava indenter (Fig. 10). The Sugluk block only became a prominent source for the Belcher basin during the deposition of the Loaf Formation after ca. 1835 Ma.

## CRediT authorship contribution statement

**Brayden S. McDonald:** Conceptualization, Formal analysis, Funding acquisition, Investigation, Methodology, Resources, Validation, Visualization, Writing – original draft, Writing – review & editing. **Camille A. Partin:** Conceptualization, Formal analysis, Funding acquisition, Project administration, Resources, Supervision, Writing – original draft, Writing – review & editing.

## Declaration of competing interest

The authors declare that they have no known competing financial interests or personal relationships that could have appeared to influence the work reported in this paper.

## Acknowledgments

This research was supported by Natural Sciences and Engineering Research Council (NSERC) grants to CAP (RGPIN-2016-04501, RGPNS-488984-2016) and the Northern Scientific Training Program to BSM. Field research was enabled by the help and friendship of the residents of Sanikiluaq NU, the Arctic Eider Society, as well as field assistants from the University of Saskatchewan including Z. Morrow-Pollock, K. Klymyshyn, and B. MacRae. Laboratory technicians at Memorial University (M. Wälle and R. Lam) and Saskatchewan Research Council (S. Creighton) are thanked for their guidance and assistance. Reviewers Don Davis and Malcolm Hodgskiss are thanked for their constructive comments that improved the manuscript.

## Appendix A. Supplementary data

Fig. S1 – Measured stratigraphic sections with the approximate location of the analyzed samples. Section locations are shown in Fig. 2 of the main text. Fig. S2 – Backscatter electron image of the three youngest detrital zircon grains used in the maximum depositional age calculation. Blue circles approximate the size and location of the ablated spot used for analysis via LA-ICP-MS. Fig. S3 – Kolmogorov–Smirnov (KS) test and multidimensional scaling (MDS) plots showing the relative similarities among the analyzed lower and middle Belcher Group sample (Costello) to previously published data (B). Comparison of the three measured upper Belcher Group samples to a previously published Loaf Formation sample demonstrating the similarities in detrital zircon populations. Fig. S4 – Elemental discrimination diagrams of Th/Yb vs. Nb/Yb and $TiO_2$ vs. Nb/Yb used to determine the role of crustal contamination (A) and melting temperatures (B) for the Flaherty Formation and Haig intrusions. Fig. S5 – Concordia diagram from LA-ICP-MS zircon analyses. Table S1: U-Pb and Lu-Hf LASS-ICP-MS results. Table S2: Single grain provenance sources for the lower and middle Belcher Group. Table S3: Single grain provenance sources for the upper Belcher Group. Supplementary data to this article can be found online at https://doi.org/10.1016/j.gr.2025.01.004.

## References


Andersson, U.B., Begg, G.C., Griffin, W.L., Högdahl, K., 2011. Ancient and juvenile components in the continental crust and mantle: Hf isotopes in zircon from Svecofennian magmatic rocks and rapakivi granites in Sweden. Lithosphere 3, 409–419.

Ansdell, K.M., 2005. Tectonic evolution of the Manitoba-Saskatchewan segment of the Paleoproterozoic Trans-Hudson Orogen. Canada. Can. J. Earth Sci. 42, 741–759.

Ansdell, K.M., Lucas, S.B., Connors, K., Stern, R.A., 1995. Kisseynew metasedimentary gneiss belt, Trans-Hudson orogen (Canada): Back-arc origin and collisional inversion. Geology 23, 1039–1043.

Ashton, K.E., Heaman, L.M., Lewry, J.F., Hartlaub, R.P., Shi, R., 1999. Age and origin of the Jan Lake Complex: a glimpse at the buried Archean craton of the Trans-Hudson Orogen. Can. J. Earth Sci. 36, 185–208.

Ashton, K.E., Lewry, J.F., Heaman, L.M., Hartlaub, R.P., Stauffer, M.R., Tran, H.T., 2005. The pelican thrust zone: basal detachment between the archean sask craton and paleoproterozoic flin flon glennie complex, western trans-hudson orogen. Can. J. Earth Sci. 42, 685–706.

Aspler, L.B., Wisotzek, I.E., Chiarenzelli, J.R., Losonczy, M.F., Cousens, B.L., McNicoll, V. J., Davis, W.J., 2001. Paleoproterozoic intracratonic basin processes, from breakup of Kenorland to assembly of Laurentia: Hurwitz Basin, Nunavut, Canada. Sed. Geol. 141–142, 287–318.

Baragar, W.R.A., 2007. 2114A, Geology Sleeper Islands, Eastern Hudson Bay. Nunavut, Geological Survey of Canada.

Baragar, W.R.A., Scoates, R.F.J., 1981. Chapter 12 The Circum-Superior Belt: A Proterozoic Plate Margin? In: Kröner, A. (Ed.), Precambrian Res. Elsevier, pp. 297–330.

Barham, M., Kirkland, C.L., Handoko, A.D., 2022. Understanding ancient tectonic settings through detrital zircon analysis. Earth and Planet. Sci. Lett. 583, 117425.

Berman, R.G., Davis, W.J., Pehrsson, S., 2007. Collisional Snowbird tectonic zone resurrected: Growth of Laurentia during the 1.9 Ga accretionary phase of the Hudsonian orogeny. Geology 35, 911–914.

Bickford, M.E., Mock, T.D., Steinhart Iii, W.E., Collerson, K.D., Lewry, J.F., 2005. Origin of the Archean Sask craton and its extent within the Trans-Hudson orogen: evidence from Pb and Nd isotopic compositions of basement rocks and post-orogenic intrusions. Can. J. Earth Sci. 42, 659–684.

Bjorkman, K.E., 2017. 4D Crust-mantle evolution of the western Superior Craton: implications for Archaean granite-greenstone petrogenesis and geodynamics. The University of Western Australia, Australia.

Black, L.P., Kamo, S.L., Allen, C.M., Davis, D.W., Aleinikoff, J.N., Valley, J.W., Mundil, R., Campbell, I.H., Korsch, R.J., Williams, I.S., Foudoulis, C., 2004. Improved 206Pb/238U microprobe geochronology by the monitoring of a trace-element-related matrix effect; SHRIMP, ID–TIMS, ELA–ICP–MS and oxygen isotope documentation for a series of zircon standards. Chem. Geol. 205, 115–140.

Boily, M., Leclair, A., Maurice, C., Bédard, J.H., David, J., 2009. Paleo- to Mesoarchean basement recycling and terrane definition in the Northeastern Superior Province, Québec, Canada. Precambrian Res. 168, 23–44.

Bouvier, A., Vervoort, J.D., Patchett, P.J., 2008. The Lu–Hf and Sm–Nd isotopic composition of CHUR: Constraints from unequilibrated chondrites and implications for the bulk composition of terrestrial planets. Earth and Planet. Sci. Lett. 273, 48–57.

Buchan, K.L., Goutier, J., Hamilton, M.A., Ernst, R.E., Matthews, W.A., 2007. Paleomagnetism, U–Pb geochronology, and geochemistry of Lac Esprit and other dyke swarms, James Bay area, Quebec, and implications for Paleoproterozoic deformation of the Superior Province. Can. J. Earth Sci. 44, 643–664.

Busby, C., Azor, A.P., 2011. Tectonics of Sedimentary Basins: Recent Advances. John Wiley & Sons.

Cawood, P.A., Hawkesworth, C.J., Dhuime, B., 2012. Detrital zircon record and tectonic setting. Geology 40, 875–878.

Chandler, F.W., Parrish, R.R., 1989. Age of the Richmond Gulf Group and implications for rifting in the Trans-Hudson Orogen, Canada. Precambrian Res. 44, 277–288.

Chauvel, C., Arndt, N.T., Kielinzcuk, S., Thom, A., 1987. Formation of Canadian 1.9 Ga old continental crust. I: Nd isotopic data. Can. J. Earth Sci. 24, 396–406.

Chiarenzelli, J., Aspler, L., Villeneuve, M., Lewry, J., 1998. Early Proterozoic evolution of the Saskatchewan Craton and its allochthonous cover, Trans-Hudson Orogen. J. Geol. 106, 247–268.

Ciborowski, T.J.R., Minifie, M.J., Kerr, A.C., Ernst, R.E., Baragar, B., Millar, I.L., 2017. A mantle plume origin for the Palaeoproterozoic Circum-Superior Large Igneous Province. Precambrian Res. 294, 189–213.

Cleven, N.R., Guilmette, C., Davis, D.W., Côté-Roberge, M., 2020. Geodynamic significance of Neoarchean metasedimentary belts in the Superior Province: Detrital zircon U-Pb LA-ICP-MS geochronology of the Opinaca and La Grande subprovinces. Precambrian Res. 347, 105819.

Corrigan, D., Galley, A.G., Pehrsson, S., Goodfellow, W.D., 2007. Tectonic evolution and metallogeny of the southwestern Trans-Hudson Orogen. Geological Association of Canada, Mineral Deposits Division 881–902.

Corrigan, D., Pehrsson, S., Wodicka, N., de Kemp, E., 2009. The Palaeoproterozoic Trans-Hudson Orogen: a prototype of modern accretionary processes. Geol. Soc. Spec. Publ. 327, 457–479.

Corrigan, D., van Rooyen, D., Wodicka, N., 2021. Indenter tectonics in the Canadian Shield: A case study for Paleoproterozoic lower crust exhumation, orocline development, and lateral extrusion. Precambrian Res. 355.

Davis, D.W., Amelin, Y., Nowell, G.M., Parrish, R.R., 2005. Hf isotopes in zircon from the western Superior province, Canada: Implications for Archean crustal development and evolution of the depleted mantle reservoir. Precambrian Res. 140, 132–156.

Demoulin, C., Lara, Y., Cornet, L., François, C., Baurain, D., Wilmotte, A., Javaux, E., 2019. Cyanobacteria evolution: Insight from the fossil record. Free Radical Biology and Medicine 140.

Dhuime, B., Hawkesworth, C., Cawood, P., 2011. When Continents Formed. Science 331, 154–155.

Dimroth, E., Baragar, W.R.A., Bergeron, R., Jackson, G.D., 1970. The filling of the Circum-Ungava geosyncline. In: Baer, A.J. (Ed.), Symposium on Basins and Geosynclines of the Canadian Shield, Paper 70-40. Geological Survey of Canada, pp. 45–142.

Dunphy, J.M., Ludden, J.N., 1998. Petrological and geochemical characteristics of a Paleoproterozoic magmatic arc (Narsajuaq terrane, Ungava Orogen, Canada) and comparisons to Superior Province granitoids. Precambrian Res. 91, 109–142.

Eglington, B.M., 2004. DateView: a windows geochronology database. Comput. Geosci. 30, 847–858.

Ernst, R.E., Bell, K., 2010. Large igneous provinces (LIPs) and carbonatites. Min. Petrol. 98, 55–76.

Ernst, R.E., Buchan, K.L., 2004. Igneous rock associations in Canada 3. Large Igneous Provinces (LIPs) in Canada and adjacent regions: 3 Ga to present. Geosci. Can. 31, 103–126.

Fisher, C.M., Hanchar, J.M., Samson, S.D., Dhuime, B., Blichert-Toft, J., Vervoort, J.D., Lam, R., 2011. Synthetic zircon doped with hafnium and rare earth elements: A reference material for in situ hafnium isotope analysis. Chem. Geol. 286, 32–47.

Gamberi, F., Rovere, M., Marani, M.P., Dykstra, M., 2015. Modern submarine canyon feeder-system and deep-sea fan growth in a tectonically active margin (northern Sicily). Geosphere 11, 307–319.

Gärtner, A., Linnemann, U., Sagawe, A., Hofmann, M., Ullrich, B., Kleber, A., 2013. Morphology of zircon crystal grains in sediments–characteristics, classifications, definitions Morphologie von Zirkonen in Sedimenten–Merkmale. Klassifikationen, Definitionen.
Hamilton, M.A., Buchan, K.L., Ernst, R.E., Scott, G.M., 2009. Widespread and short-lived 1870 Ma mafic magmatism along the northern Superior Craton margin, in: GA08. Presented at the American Geophysical Union–Geological Association of Canada–Mineralogical Association of Canada, Joint Assembly 2009, Toronto, Ontario.
Hegner, E., Bevier, M.L., 1991. Nd and Pb isotopic constraints on the origin of the Purtuniq ophiolite and Early Proterozoic Cape Smith Belt, northern Québec. Canada. Chem. Geol. 91, 357–371.
Hodgskiss, M.S.W., Dagnaud, O.M.J., Frost, J.L., Halverson, G.P., Schmitz, M.D., Swanson-Hysell, N.L., Sperling, E.A., 2019. New insights on the Orosirian carbon cycle, early Cyanobacteria, and the assembly of Laurentia from the Paleoproterozoic Belcher Group. Earth and Planet. Sci. Lett. 520, 141–152.
Hoffman, P., 1981. Autopsy of Athapuscow aulacogen: a failed arm affected by three collisions, in. Proterozoic Basins of Canada 97–102.
Hoffman, P.F., 1988. United Plates of America, The Birth of a Craton: Early Proterozoic Assembly and Growth of Laurentia. Annu. Rev. Earth Planet. Sci. 16, 543–603.
Hoffman, P.F., 1990. Subdivision of the Churchill Province and the extent of the Trans-Hudson Orogen. The Early Proterozoic Trans-Hudson Orogen of North America 15–39.
Hofmann, H.J., 1976. Precambrian Microflora, Belcher Islands, Canada: Significance and Systematics. J. Paleontol. 50, 1040–1073.
Jackson, G.D., 1960. Belcher Islands, Northwest Territories, 33M, 34D, E. Geological Survey of Canada, Paper 60–20, 13.
Jackson, G.D., 2013. Geology, Belcher Islands. Nunavut, Geological Survey of Canada, p. 159.
Ketchum, J.W.F., Jackson, S.E., Culshaw, N.G., Barr, S.M., 2001. Depositional and tectonic setting of the Paleoproterozoic Lower Aillik Group, Makkovik Province, Canada: evolution of a passive margin-foredeep sequence based on petrochemistry and U–Pb (TIMS and LAM-ICP-MS) geochronology. Precambrian Res. 105, 331–356.
Kinny, P.D., Maas, R., 2003. Lu–Hf and Sm–Nd isotope systems in zircon. RiMG 53, 327–341.
Legault, F., Francis, D., Hynes, A., Budkewitsch, P., 1994. Proterozoic continental volcanism in the Belcher Islands: implications for the evolution of the Circum Ungava Fold Belt. Can. J. Earth Sci. 31, 1536–1549.
Lewry, J.F., 1990. The Trans-Hudson Orogen: extent, subdivision, and problems. The Early Proterozoic Trans-Hudson Orogen of North America 1–14.
Li, D., Hollings, P., Chen, H., Sun, X., Tan, C., Zurevinski, S., 2020. Zircon U–Pb and Lu–Hf systematics of the major terranes of the Western Superior Craton, Canada: Mantle-crust interaction and mechanism(s) of craton formation. Gondwana Res. 78, 261–277.
Lucas, S.B., 1989. Structural evolution of the Cape Smith Thrust Belt and the role of out-of-sequence faulting in the thickening of mountain belts. Tectonics 8, 655–676.
Lucas, S.B., Stern, R.A., Syme, E.C., Reilly, B.A., Thomas, D.J., 1996. Intraoceanic tectonics and the development of continental crust: 1.92–1.84 Ga evolution of the Flin Flon Belt. Canada. Geol. Soc. Am. Bull. 108, 602–629.
Martins, T., Rayner, N., Corrigan, D., Kremer, P., 2022. Regional geology and tectonic framework of the Southern Indian domain, Trans-Hudson orogen. Manitoba. Can. J. Earth Sci. 59, 371–388.
McDonald, B., Partin, C., 2024. Paleoproterozoic Rocks of the Belcher Islands, Nunavut: A Review of Their Remarkable Geology and Relevance to Inuit-led Conservation Efforts. Geosci.can. 51, 7–42.
Meek, D.M., Mole, D.R., Fernandes, B.A., 2020. Metal Earth Geochronology Compilation: Superior Craton and surrounding area (No. MERC-ME-2020-073). Laurentian University Mineral Exploration Research Centre.
Mole, D.R., Thurston, P.C., Marsh, J.H., Stern, R.A., Ayer, J.A., Martin, L.A.J., Lu, Y.J., 2021. The formation of Neoarchean continental crust in the south-east Superior Craton by two distinct geodynamic processes. Precambrian Res. 356, 106104.
Morrow-Pollock, Z., 2021. The Geobiology of the Paleoproterozoic Belcher Group. University of Saskatchewan, Nunavut, Canada. PhD Thesis.
Pehrsson, S.J., Berman, R.G., Davis, W.J., 2013. Paleoproterozoic orogenesis during Nuna aggregation: a case study of reworking of the Rae craton, Woodburn Lake, Nunavut. Precambrian Res. 232, 167–188.
Percival, J.A., 2007. Geology and metallogeny of the Superior Province, Canada. In: Mineral Deposits of Canada: A Synthesis of Major Deposit-Types, District Metallogeny, the Evolution of Geological Provinces, and Exploration Methods. Geological Association of Canada, Mineral Deposits Division. Special Paper, pp. 903–928.
Polat, A., Frei, R., Deng, H., Yang, X.-M., Sotiriou, P., 2022. Anatomy of a Neoarchean continental arc-backarc system in the Cross Lake-Pipestone Lake region, northwestern Superior Province, Canada. Precambrian Res. 370, 106556.
Rasmussen, B., Fletcher, I.R., Bekker, A., Muhling, J.R., Gregory, C.J., Thorne, A.M., 2012. Deposition of 1.88-billion-year-old iron formations as a consequence of rapid crustal growth. Nature 484, 498–501.
Rayner, N.M., Stern, R.A., Bickford, M.E., 2005. Tectonic implications of new SHRIMP and TIMS U Pb geochronology of rocks from the Sask Craton, Peter Lake Domain, and Hearne margin, Trans-Hudson Orogen, Saskatchewan. Can. J. Earth Sci. 42, 635–657.
Ricketts, B., 1979. Sedimentology and stratigraphy of eastern and central Belcher Islands. Carelton University, Ottawa, Canada, Northwest Territories.
Ricketts, B.D., 1981. A Submarine Fan - Distal Molasse Sequence of Middle Precambrian Age, Belcher Islands, Hudson Bay. Bull. Can. Pet. Geol. 29, 561–582.
Ricketts, B.D., 1983. The evolution of a middle Precambrian dolostone sequence; a spectrum of dolomitization regimes. J. Sediment. Res. 53, 565–586.
Ricketts, B.D., Donaldson, J.A., 1988. Stromatolite Reef Development on a Mud-Dominated Platform in the Middle Precambrian Belcher Group of Hudson Bay 113–119.
Ricketts, B.D., Donaldson, J.A., 1981. Sedimentary history of the Belcher Group of Hudson Bay. Proterozoic Basins of Canada 81, 235–254.
Ricketts, B.D., Ware, M.J., Donaldson, J.A., 1982. Volcaniclastic rocks and volcaniclastic facies in the Middle Precambrian (Aphebian) Belcher Group, Northwest Territories. Canada. Can. J. Earth Sci. 19, 1275–1294.
Sherman, A.G., 1994. Anatomy of Giant Stromatolite Mounds in the Paleoproterozoic Mavor Formation. Belcher Islands, NWT.
Sláma, J., Košler, J., Condon, D.J., Crowley, J.L., Gerdes, A., Hanchar, J.M., Horstwood, M.S.A., Morris, G.A., Nasdala, L., Norberg, N., Schaltegger, U., Schoene, B., Tubrett, M.N., Whitehouse, M.J., 2008. Plešovice zircon — A new natural reference material for U–Pb and Hf isotopic microanalysis. Chem. Geol. 249, 1–35.
Smith, A.D., Ludden, J.N., 1989. Nd isotopic evolution of the Precambrian mantle. Earth and Planet. Sci. Lett. 93, 14–22.
Stern, R.A., Syme, E.C., Bailes, A.H., Lucas, S.B., 1995. Paleoproterozoic (1.90–1.86 Ga) arc volcanism in the Flin Flon Belt, Trans-Hudson Orogen, Canada. Contrib, Mineral. Petrol. 119, 117–141.
Stevenson, R.K., David, J., Parent, M., 2006. Crustal evolution of the western Minto Block, northern Superior Province, Canada. Precambrian Res. 145, 229–242.
St-Onge, M.R., Ijewliw, O.J., 1996. Mineral corona formation during high-P retrogression of granulitic rocks, Ungava Orogen, Canada. J. Petrol. 37, 553–582.
St-Onge, M.R., Gool, J.A.M.V., Garde, A.A., Scott, D.J., 2009. Correlation of Archaean and Palaeoproterozoic units between northeastern Canada and western Greenland: constraining the pre-collisional upper plate accretionary history of the Trans-Hudson orogen. Geol. Soc. Spec. Publ. 318, 193–235.
St-Onge, M.R., Lucas, S.B., 1991. Evolution of regional metamorphism in the Cape Smith Thrust Belt (northern Quebec, Canada): interaction of tectonic and thermal processes. J. Metamorph. Geol. 9, 515–534.
St-Onge, M.R., Scott, D.J., Lucas, S.B., 2000. Early partitioning of Quebec: Microcontinent formation in the Paleoproterozoic. Geology 28, 323–326.
St-Onge, M.R., Searle, M.P., Wodicka, N., 2006. Trans-Hudson Orogen of North America and Himalaya-Karakoram-Tibetan Orogen of Asia: Structural and thermal characteristics of the lower and upper plates. Tectonics 25.
Vervoort, J.D., Plank, T., Prytulak, J., 2011. The Hf–Nd isotopic composition of marine sediments. Geochim. Cosmochim. Acta 75, 5903–5926.
Weller, O.M., St-Onge, M.R., 2017. Record of modern-style plate tectonics in the Palaeoproterozoic Trans-Hudson orogen. Nat. Geosci. 10, 305–311.
Whalen, J.J., Pehrsson, S.J., Rayner, N.M., 2016. Significance of pre-1860 Ma granitoid magmatism for crustal evolution and exploration targeting in the Flin Flon assemblage, Trans-Hudson orogen. Canada. Econ. Geol. 111, 1021–1039.
Whalen, J.B., Syme, E.C., Stern, R.A., 1999. Geochemical and Nd isotopic evolution of Paleoproterozoic arc-type granitoid magmatism in the Flin Flon Belt, Trans-Hudson orogen. Canada. Can. J. Earth Sci. 36, 227–250.
White, D.J., Lucas, S.B., Bleeker, W., Hajnal, Z., Lewry, J.F., Zwanzig, H.V., 2002. Suture-zone geometry along an irregular Paleoproterozoic margin: The Superior boundary zone, Manitoba, Canada. Geology 30, 735–738.
Wiedenbeck, M., Allé, P., Corfu, F., Griffin, W. l., Meier, M., Oberli, F., Quadt, A.V., Roddick, J. c., Spiegel, W., 1995. Three Natural Zircon Standards for U-Th-Pb, Lu-Hf, Trace Element and Ree Analyses. GeoStan. News 19, 1–23.
Woodhead, J.D., Hergt, J.M., 2005. A Preliminary Appraisal of Seven Natural Zircon Reference Materials for In Situ Hf Isotope Determination. Geostand. Geoanal. Res. 29, 183–195.
Zwanzig, H.V., Lewry, J.F., Stauffer, M.R., 1990. Kisseynew gneiss belt in Manitoba: stratigraphy, structure, and tectonic evolution. The Early Proterozoic Trans-Hudson Orogen of North America. Edited by JF Lewry and MR Stauffer. Geological Association of Canada, Special Paper 37, 95–120.